Spring 2014

Corrosion resistance of enamel coating modified by calcium silicate and sand particle for steel reinforcement in concrete

Fujian Tang

Department:

CORROSION RESISTANCE OF ENAMEL COATING MODIFIED BY CALCIUM SILICATE AND SAND PARTICLE FOR STEEL REINFORCEMENT IN CONCRETE

by

FUJIAN TANG

A THESIS

Presented to the Faculty of the Graduate School of the

MISSOURI UNIVERSITY OF SCIENCE AND TECHNOLOGY

In Partial Fulfillment of the Requirements for the Degree

MASTER OF SCIENCE

IN

MATERIALS SCIENCE AND ENGINEERING

2014

Approved by

Richard K. Brow, Advisor
Genda Chen, Co-advisor
William G. Fahrenholtz

PUBLICATION THESIS OPTION

This thesis has been prepared in the style utilized by Construction and Building Materials. It consists of two papers, the first paper (pages 21-50) has been published in the journal, and the second paper (pages 51-77) is intended for submission.

ABSTRACT

Porcelain enamel has stable chemical property in harsh environments such as high temperature, acid and alkaline, and it can also chemically react with substrate reinforcing steel resulting in improved adherence strength. In this study, the corrosion resistances of enamel coating modified by calcium silicate and sand particles, which are designed for improved bond strength with surrounding concrete, were investigated in 3.5 wt% NaCl solution. It consists of two papers that describe the results of the study.

The first paper investigates the corrosion behavior of enamel coating modified by calcium silicate applied to reinforcing steel bar in 3.5 wt% NaCl solution by OCP, electrochemical impedance spectroscopy (EIS) and potentiodynamic polarization. The coatings include a pure enamel, a mixed enamel that consists of 50% pure enamel and 50% calcium silicate by weight, and a double enamel that has an inner pure enamel layer and an outer mixed enamel layer. Electrochemical tests demonstrates that both pure and double enamel coatings can significantly improve corrosion resistance, while the mixed enamel coating offers very little protection due to connected channels.

The second paper is focused on the electrochemical characteristics of enamel coating modified by sand particle applied to reinforcing steel bar in 3.5 wt% NaCl solution by EIS. Six percentages by weight are considered including 5%, 10%, 20%, 30%, 50%, and 70%. Results reveal that addition of sand particle does not affect its corrosion resistance significantly. Most of the sand particles can wet very well with enamel body, while some have a weak zone which is induced during the cooling stage due to different coefficient of thermal expansion. Therefore, quality control of sand particle is the key factor to improve its corrosion resistance.

ACKNOWLEDGEMENTS

The author would like to express his sincere gratitude to his advisor Dr. Richard K. Brow, and co-advisor, Dr. Genda Chen, for their continuing support, encouragement and invaluable advice throughout this research work. He would like to thank Dr. Fahrenholtz for serving as his committee member and for the time in which he had spent reviewing this thesis.

Financial support to complete this study was provided by the U.S. National Science Foundation under the Award No. CMMI-0900159, the Missouri Department of Transportation under the Award No. 28015485-09R000587, and the Center for Transportation Infrastructure and Safety at Missouri University of Science and Technology under the Award No. DTRT06-G-0014. The results and opinions expressed in this thesis are those of the author only and don't necessarily represent those of the sponsors.

The author would like to thank Signo Reis, Xiaoming Cheng, Eric Bohannan, Clarissa Wisner, for their help to characterize enamel coating using XRD, SEM, and other instruments. He would also like to thank Denise Eddings for looking out for his academic well-being.

The author wishes to express his special and sincere gratitude to his parents for their love, understanding and encouragement to pursue his degree. And the author would like to express his sincere gratitude to his aunt Josephine Chain for her encouragement during his study in the U.S.

TABLE OF CONTENTS

LIST OF ILLUSTRATIONS

PAPER II

LIST OF TABLES

1. INTRODUCTION

1.1 HISTORY, CONSTITUENTS, AND APPLICATION OF ENAMEL

The technique of enameling dates back to over 3000 years ago, when it was used to decorate the surfaces of objects for aesthetic purposes. With advent of industrial revolution, it began to be used as a coating material applied to iron and steel for other purposes, such as corrosion protection, heat resistance, abrasion resistance, hygiene, and so on [1-4]. Today, enamel is widely used in domestic appliances, industrial environments and the construction industry. In the home, cooking utensils like hot dishes, cooking ware [5, 6], oven, and so on, are coated with enamel, because it is easy to clean, can prevent the growth of bacteria, does not absorb odors, and is not attacked by food acids. In industry, it is commonly used as a protective coating in harsh environments such as acid, alkaline, high temperature for the interior protection of tanks, boilers, ovens, tubes and stove components [7, 8], because of its chemical inertness. In construction industry, enamel is used as decoration for cladding buildings or for interior decoration, as it combines a rigid steel substrate with various surface effects such as texture, reflectivity, salt and pepper effects and metallized colors.

Enamel is a glass obtained by fusion at high temperature between 1000°C and 1300°C, and the main constituent in enamel is silica with is the most abundant material in the earth's crust. In order to change its property for specific application, other materials are added. In general, the raw materials used in enamel can be divided into six groups, namely, refractories, fluxes, opacifiers, colors, floating agents, and electrolytes [1]. Refractories help in the development of the enamel's structure and mechanical strength, and these include quartz, feldspar, clay, and alumina. Alumina (Al_2O_3) is a common

refractory oxide that increases the enamel's resistance to temperature, chemical attack, and abrasion. Fluxes are used to react with refractories to form the glass, these include borax, soda ash, cryollite, and fluorspar. Other oxides containing sodium (Na_2O), potassium (K_2O), lithium (Li_2O), calcium (CaO), and magnesium (MgO) are also used as a fluxing agent [1]. Adhesion agents are added to an enamel to promote the adhesion between the enamel and the steel. These oxides include nickel (NiO), molybdenum (MoO_2), cobalt (Co_3O_4), cupric (CuO), manganese (MnO_2) and chromic oxides (Cr_2O_3). Opacifiers serve in the development of enamel's visual qualities. The commonly used opacifiers include titanium dioxide (TiO_2), antimony oxide (Sb_2O_5), zirconium oxide (ZrO_2), and tin oxide (SnO_2). The color materials produce different colors, these may be oxides, elements, or salts. The floating agents are mill additions which are used to suspend the enamel in water or some other liquid, and these include clay, gums, bentonite, and others.

Enamel may be applied to a steel surface using either the wet or dry process. The wet process needs preparation of enamel slurry. In the wet process, steel is dipped into a vat containing enamel slurry or enamel slurry is sprayed upon the surface of the steel using air-assisted spraying or electrostatic spraying. The dry application is carried out by applying an electric field between the nozzle electrode and the part to be enameled, and it uses enamel particles instead of enamel slurry.

Now, one layer or two layer enamels are commonly used. The two layer enamel includes a ground coat enamel and a cover coat enamel. The ground coat enamel ensures the adherences between the coating and the substrate [9-11], and it usually contains metal oxides such as NiO, CoO, and CuO. The ground-coat enamel can also protect against

aggressive environments, for example, addition of TiO_2 increases acid resistance, use of ZrO_2 enhances alkaline resistance, and application of ZrO_2 and Al_2O_3 improves corrosion resistance for water-heater applications [12]. The cover coat enamel mainly provides different surface properties [2].

1.2 RESEARCH OBJECTIVES

The main objective of this study is to characterize the corrosion resistance of enamel coatings modified by calcium silicate and sand particles, which are designed to increase the bond strength of reinforcing steel bar with surrounding concrete in reinforced concrete (RC) structures. Addition of calcium silicate can increase the bond strength between enamel coating and concrete by chemical reaction, typically chemical bond. The use of sand particles can enhance the bond strength by mechanical interlocking with surrounding concrete due to increased surface roughness. The scientific contributions of this research are described in two manuscripts that make up the body of the thesis.

Paper I. The first paper investigated the effect of additions of calcium silicate to enamel coatings on the microstructure and corrosion properties. Three types of enamels were developed with different purposes: pure enamel is a commercially available products which is used to increase the corrosion resistance as a coating, mixed enamel is made of mixing 50% of calcium silicate from Portland cement with 50% of pure enamel, which is designed to chemically bond to the surrounding concrete for enhanced bond strength; double enamel is a two layer coating with an inner layer of pure enamel to increase corrosion resistance and outer layer of mixed enamel to enhance bond strength.

Paper II. The second paper studied the electrochemical characteristics of coatings modified by sand particle with EIS. Six percentages of sand particles by weight were

investigated: 5%, 10%, 20%, 30%, 50%, and 70%. Effects of sand particle on the surface and cross sectional morphologies were characterized with scanning electron microscopy (SEM). In the end, the electrochemical results were also compared with sample modified by calcium silicate.

2. LITERATURE REVIEW

2.1 CORROSION OF STEEL IN CONCRETE

Reinforcement steel in concrete structures is generally protected by a passive film which is formed due to the highly alkaline environment of the fresh concrete. However, this protective film can be destroyed by penetration of carbon dioxide or aggressive ions such as chloride. Therefore, two types of corrosion commonly occur in RC structures.

2.1.1 Carbonation-induced Corrosion. When carbon dioxide diffuses into concrete, in the presence of water, it reacts with calcium hydroxide to form calcium carbonate as shown in Equation (2.1). As a result, the pH of the pore solution is reduced. A reduction in the pH value of pore solution below 8.3 causes depassivation of the steel bars and initiation of corrosion, due to dissolution of the protective passive film. This process is called carbonation-induced corrosion. The evolution of the concrete carbonation processes with time depends on the composition of the concrete and the environmental conditions. The main compositional parameters of concrete are the chemical composition of cement, the water to cement ratio, and aggregate to cement ratio of the concrete. The main environmental factors are the ambient CO_2 concentration and the ambient relative humidity.

$$CO_2 + Ca(OH)_2 \rightarrow CaCO_3 + H_2O \quad (2.1)$$

Carbonation is controlled by the ingress of carbon dioxide into the concrete pore system by diffusion, with a concentration gradient acting as a driving force [13].

Therefore, the carbonation rate is diffusion-controlled and the diffusion coefficient for carbon dioxide in carbonated concrete is the characteristic transport coefficient. Assuming a constant diffusion coefficient for the carbonated concrete layer, the depth of carbonation can be derived from Fick's first law of diffusion approximated by:

$$\frac{dx}{dt} = \frac{D}{x} \tag{2.2}$$

where x is the distance of carbonation front to the surface, t is time, and D is a diffusion coefficient [14]. However, the application of Fick's first law of diffusion using constant parameters has limitations, because D varies with location x and is strongly dependent on the moisture content in the concrete pores.

Experimental studies have been carried out and empirical equation or models have been proposed to describe the carbonation process of concrete. Experimental studies on carbonation of various fly ash concretes under laboratory and atmospheric conditions were conducted by Thomas and Matthews [15]. Recent accelerated carbonation and weathering studies were reported by Roy et al. [16]. Brieger and Wittmann [17] set up a model for the carbonation reaction, and it was combined with a one-dimensional diffusion model for heat, moisture and CO_2 flow by Saetta et al. [18] who proposed a two-dimensional extension later [19]. Jiang et al. [20] proposed a mathematical model for carbonation of high-volume fly ash concrete. Papadakis et al. [21] proposed a simple mathematical model for the evolution of carbonation over time. Steffens et al. [22] developed a theoretical model to predict carbonation of concrete structures by means of balanced equations and diffusion laws.

2.1.2 Chloride-induced Corrosion. Chlorides exist in concrete in two forms: free and bound. When free chloride ions from environmental solutions penetrate into the concrete, some of them will be captured by the cement hydration products, which is called “chloride binding”. The other chloride ions that are not captured will continue to transport into concrete. In general, chloride transport in concrete is a rather complicated process, which involves ion diffusion, capillary suction and convective flow with flowing water, accompanied by physical and chemical binding. Sometimes, the mechanism of migration is involved in the presence of external electrical potential [23].

Diffusion is the movement of a substance under a gradient of concentration or, more strictly speaking, chemical potential, from an area of high concentration to an area of low concentration. When a chloride gradient exists within the concrete and pore solution is present, chloride ions may then diffuse through the concrete. To understand the chloride transport mechanism, Fick’s second diffusion law [24] was used to simulate the diffusion process of chloride ions. In this case, the flux of chlorides at any time is proportional to the gradient of chloride concentration in the mortar of semi-infinite medium. That is,

$$\frac{\partial C}{\partial t} = D_a \frac{\partial^2 C}{\partial x^2} \tag{2.3}$$

from which an analytical solution can be derived and expressed into [25]:

$$C_x = C_s \left[1 - erf\left(\frac{x}{2\sqrt{D_a t}} \right) \right] \tag{2.4}$$

where x represents the depth from the surface of the mortar cylinder, t denotes the exposure time, C_x is the chloride ion concentration at depth of x after an exposure time t, C_s is the chloride ion concentration at the surface of the mortar specimen, D_a is the apparent chloride diffusion coefficient, and erf represents the Gaussian error function.

Over the last fifty years, a considerable amount of papers has been published presenting values for critical chloride content in reinforced concrete, because critical chloride content is one of the most important input parameters to predict initiation of corrosion due to arrival of chloride at the steel surface. For example, Augst et al. [26] summarized the state of the art by presenting the concept of the critical chloride content, discussing influencing factors, and assessing available measurement techniques. Ann et al. [27, 28] discussed the critical threshold level of chloride for steel corrosion in concrete as well as the importance of chloride content at the concrete surface. And Poupard et al [29] studied the chloride action on depassivation of a steel bar in cement based material and quantified the chloride concentration threshold by use of impedance spectroscopy. Yu et al. [30] experimentally investigated the chloride threshold content for a series of self-compacting concrete and regular concretes.

2.2 CORROSION TEST METHODS

As a result of the development of the fundamental understanding of corrosion, a lot of electrochemical techniques exist for the study of corrosion. It is not the purpose of this thesis to present a comprehensive summary of electrochemical methods for corrosion measurement, thus just three commonly used methods are addressed.

2.2.1 Open-circuit Potential. Corrosion of steel is a process of two main electrochemical reactions: oxidation of steel and reduction of oxygen, which are represented by equations (2.5) and (2.6), respectively. The so-called half-cell potential represents the mixed potential of these two reactions, which is an important indicator of reaction activity according to the Nernst equation (2.7).

$$Fe \rightarrow Fe^{2+} + 2e^{-} \tag{2.5}$$

$$O_2 + 2H_2O + 4e^{-} \rightarrow 4OH^{-} \tag{2.6}$$

$$E_{oc} = E_0 - RT \ln([C]_p / [C]_R) / nF \tag{2.7}$$

where E_{oc} is the open-circuit potential, E_0 is the half-cell potential in standard condition, R is the gas constant, T is the absolute temperature, F is the Faraday constant, n is the number of moles of electrons transferred in the cell reaction, and $[C]_p$ and $[C]_R$ represent the concentration of corrosion products and reactants, respectively [12]. Eq. (2.7) indicates that the open-circuit potential is a function of the ratio of product concentration to reactant concentration. The higher the product concentration, the lower the open-circuit potential is. Therefore, open-circuit potential can be an indirect indicator of corrosion activity.

The measurement of the corrosion potential for RC structures is covered in ASTM C-876 [31]. It must be emphasized that the half-cell potential alone does not provide information on the corrosion rate of the specimens. According to this guideline, the probability of corrosion initiation is greater than 90% when open-circuit potentials are more negative than -350 mV relative to the copper sulfate electrode (CSE). However, this

method has some drawbacks. Theoretical considerations and practical experience have shown that the results require careful interpretation because a lot of factors can affect the measured corrosion potentials. For example, a steel bar placed within an environment lacking oxygen is capable of generating highly negative potentials that may reach beyond -350 mV which corresponds to a 90% probability that the steel is corroding. However, with a lack of oxygen, the cathodic reaction may not be established.

2.2.2 Tafel Extrapolation. This technique uses data obtained from cathodic and anodic polarization measurement. Cathodic data are preferred, since these are easier to measure experimentally. Figure 2.1 illustrates the typical polarization curve, and can be mathematically expressed as [32]:

$$i = i_{corr}\left(\exp\left[\frac{2.3(E - E_{corr})}{\beta_a}\right] - \exp\left[\frac{-2.3(E - E_{corr})}{|\beta_c|}\right]\right) \tag{2.8}$$

where i is the current measured as a function of applied potential E, E_{corr} is the corrosion potential, i_{corr} is the corrosion current density, and β_a and β_a are the anodic and cathodic Tafel slopes, respectively.

In Figure 2.1, the total cathodic curves correspond to oxygen reduction reaction (Equation 2.6) and the anodic curve corresponds to steel dissolution (Equation 2.5) interact at the corrosion potential. By linearly fitting the straight portion of the cathodic and the anodic curves, the corrosion potential can be determined. The corrosion potential corresponds to the condition that the rate of oxygen reduction is equal to the rate of steel dissolution, and at this point the corrosion rate of the system can also be determined. The

slopes of both fitted anodic and cathodic straight lines are the two Tafel constants, β_a for anodic polarization and β_c for cathodic polarization.

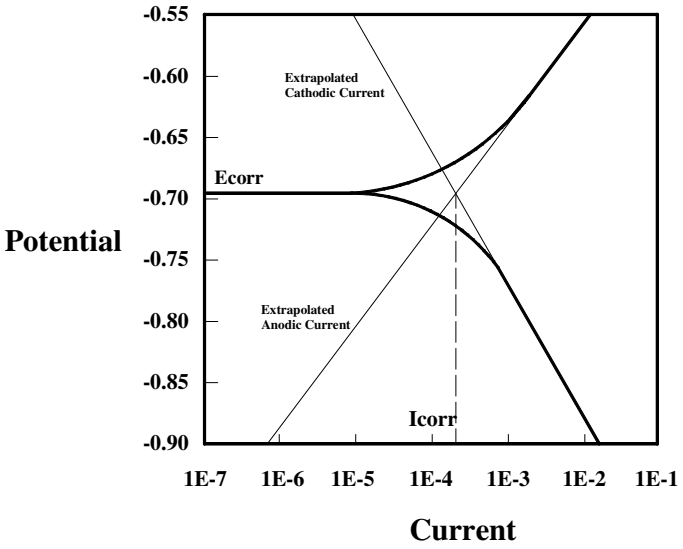

Figure 2.1 Typical polarization curve.

2.2.3 Electrochemical Impedance Spectroscopy. Electrochemical Impedance Spectroscopy (EIS) is an electrochemical technique that allows the physical properties of a material to be related to its chemical properties. EIS provides a more thorough understanding of an electrochemical system than any other electrochemical technique. Its experiment involves the application of a wide range of sinusoidal frequencies at low voltage amplitudes to a sample material. The different frequency excitations allow measurement of several electrochemical reactions that take place at very different rates as well as the measurement of the capacitance of the electrode. EIS is a powerful tool in the study of coating performance [33-37]. This technique allows the deterioration of a coating to be evaluated from the changes induced in impedance diagrams by the appearance of surface phenomena (pores or defects, delamination at metal/coating interface, water adsorption). In practice, the measured impedance information can be

modeled as an equivalent circuit which consists of a number of electrical elements such as resistors, capacitors, inductors and so on. From changes in the simulated electrical element, we can identify the changes in coatings and detect coating damage due to corrosion.

Figure 2.2 shows the typical equivalent circuit for simulation of EIS results. In this circuit, R_s represent the solution resistance, R_p is the polarization resistance or charge transfer resistance, C_{dl} or CPE_{dl} represent the double layer capacitance. Replacement of the capacitance with the constant phase element (CPE) was attributed to the non-homogeneity induced by the coating [38-41]. CPE is defined by two parameters Y and n. When n = 1, CPE resembles a capacitor with capacitance Y. When n =0, CPE represents a resistor with resistance Y^{-1}.

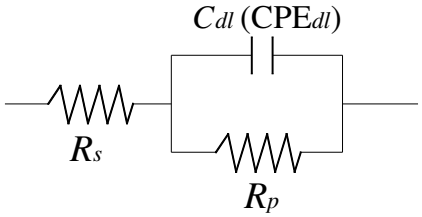

Figure 2.2 Typical equivalent circuit for EIS test.

2.3 PROTECTIVE COATINGS

Use of protective coating on reinforcement steel is one of the most effective methods to protect from corrosion, because it can establish a physical barrier between the corrosive chemicals and the reinforcement steel. The following section gives a brief summary of the two widely used protective coating on reinforcement steel: fusion bonded epoxy and hot dipped galvanized zinc.

2.3.1 Fusion Bonded Epoxy. As a protective coating for reinforcement steel in RC structures, Fusion bonded epoxy coatings were developed in the 1970s in North America. Earlier laboratory studies showed that the epoxy coating can provide effective corrosion protection to steel reinforcement in carbonated or chloride contaminated concrete [42-44]. Later, however, field surveys conducted by the Florida Department of Transportation (FDOT) discovered that ECR embedded within the substructure of several relatively new marine bridges had begun to exhibit signs of corrosion.

Protection of reinforcement steel by epoxy coating is based on the principles of acting as both a physical and electrochemical barrier. As a physical barrier, the epoxy coating prevents penetration of aggressive chloride ions and other corrosive elements, which would initiate the corrosion of steel. The coating has also shown the ability to reduce macrocell corrosion by limiting both the size and the number of locations along a bar where the cathodic reaction can occur.

The effectiveness of epoxy to prevent steel from corroding is highly dependent upon the degree to which it is adhered to the steel. Laboratory studies have shown that potassium (K) and sodium (Na) ions can expedite the debonding process, especially when breaks within the coating exist [45]. Research has also discovered that the rate of debondment increases as the relative humidity within the concrete, at a depth equal to that of the embedded ECR, reaches 60 percent or higher.

Another concern about effectiveness of epoxy coatings is initial coating imperfections and additional surface damage induced by shipping, handling and a severe construction environment. The damaged coating area provides a pathway for aggressive ions to penetrate through the epoxy and corrosion takes place on the surface of the

exposed steel. Furthermore, once initiated, corrosion can extend beneath the coating, which is called under-film corrosion [46].

2.3.2 Hot Dipped Galvanized Zinc. Galvanized steel bars can be used as a preventive measure to control corrosion in reinforced concrete structures. They are produced by the hot-dip galvanizing process. This process produces a metallic coating composed of various layers of iron-zinc alloys, which has a metallurgical adhesion to the steel substrate. The whole layer could be approximately divided into two layers, the external layer is pure zinc formed by solidification of liquid zinc, and the middle layer is iron-zinc alloy as a result of formation of brittle intermetallic compounds [47].

The protective properties of zinc coatings are due for the most part to the external layer of zinc, which can form a passive film of calcium hydroxyzincate. This passive film that formed on zinc not only reduces the rate of the anodic process (zinc dissolution), but even hinders cathodic reactions of oxygen reduction and hydrogen development [48].

Unlike epoxy coatings, defects or breaks within the protective zinc coating will not reduce the corrosion performance of galvanized steel reinforcement, because the zinc surrounding the defect will sacrificially corrode to protect the underlying steel. Because of this property, a great deal of attention must be paid when using both uncoated (bare) steel rebar and galvanized steel rebar within a structure, for an accelerated depletion of a galvanized steel bar's zinc coating may occur when it contacts with an uncoated steel bar. This coupling effect would lead to a significant reduction in the long term corrosion performance of galvanized steel rebar [14]. In addition, galvanized steel rebar have two main concerns in engineering application. First, the zinc coating corrodes vigorously due to the high alkaline environment in fresh concrete if no passive film is formed. Second,

the hydrogen produced in the cathodic reaction would increase the porosity of adjacent cement pastes and thus reduce the bond strength between the rebar and the concrete [49].

REFERENCES

[1] Andrew AI. Porcelain enamel, 2nd ed. Champaign (IL): The Garrard Press; 1961.

[2] Kuchinski FA. Corrosion resistant thick films by enamelling, In: Wachtman JB, Haber RA, editors. Ceramic films and coatings. Park Ridge (NJ): Noyes Publication; 1993, p. 77-130.

[3] Shreir LL, Jarman RA, Burstein GT. Editors, Corrosion. London: Newnes-Butterworths; 1998.

[4] Zucchelli A, Minak G, Ghelli D. Low-velocity impact behaviour of vitreous enameled steel plate. International Journal of Impact Engineering 2010; 37: 673-684.

[5] Conde A, Damborenea JJ. Electrochemical impedance spectroscopy for studing the degradation of enamel coatings. Corrosion Science 2002; 44:1555-1567.

[6] Conde A, Damborenea J. Monitoring of vitreous enamel degradation by electrochemical noise. Surface and Coatings Technology 2002; 150: 212-217.

[7] Zhou M, Li K, Shu D, Sun BD, Wang J. Corrosion resistance properties of enamels with high B2O3/P2O5 content to molten aluminium. Materials Science and Engineering: A 2003; 346: 116-121.

[8] Tang Z, Wang F, Wu W. Effect of Al2O3 and enamel coatings on 900°C oxidation and hot corrosion behaviors of gamma-TiAl. Materials Science and Engineering: A 2000; 276: 70-75.

[9] Samiee L, Sarpoolaky H, Mirhabibi A. Microstructure and adherence of cobalt containing and cobalt free enamels to low carbon steel. Materials Science and Engineering: A 2007; 458: 88-95.

[10] Yang X, Jha A, Brydson R, Cochrane RC. The effects of a nickel oxide precoat on the gas bubble structures and fish-scaling resistance in vitreous enamels. Materials Science Engineering: A 2004; 366: 254-261.

[11] Barcova K, Mashlan M, Zboril R, Filip J, Podjuklova J, Hrabovska K, Schaaf P. Phase composition of steel-enamel interfaces: effects of chemical pre-treatment. Surface and Coatings Technology 2006; 201: 1836-1844.

[12] Jones DA, Principles and prevention of corrosion, 2nd ed., Published by Prentice-Hall, Inc. Upper Saddel River, NJ, 1996.

[13] Basheer L, Kropp J, Cleland DJ. Assessment of the durability of concrete from its permeation properties: a review. Construction and Building Materials 2001; 15: 93-103.

[14] Broomfield JP. Corrosion of steel in concrete: understanding, investigation and repair. 2nd ed., Published by Taylor & Francis, 270 Madison Ave, New York, NY, 2007.

[15] Thomas MDA, Matthews JD. Carbonation of fly ash concrete, Magazine of Concrete Research 1992; 44(160): 217-228.

[16] Roy SK, Poh KB, Northwood DO. Durability of concrete-accelerated carbonation and weathering studies. Building Environments 1999; 34: 597-606.

[17] Breiger L, Wittmann FH. Numerical simulation of carbonation of concrete. Material and Science Restoration, Tech, Akad, Esslingen, Ostifildern, 1986.

[18] Saetta AV, Schrefler BA, Vitaliani R. The carbonation of concrete and the mechanism of moisture, heat and carbon dioxide flow through porous materials. Cement and Concrete Research 1993; 23:761-772.

[19] Saetta AV, Schrefler BA, Vitaliani R. 2-D model for carbonation and moisture/heat flow in porous materials. Cement and Concrete Research 1995; 25: 1703-1712.

[20] Jiang L, Lin B, Cai Y. A model for predicting carbonation of high-volume fly ash concrete. Cement and Concrete Research 2000; 30: 699-702.

[21] Papadakis VG, Fardis MN, Vayenas CG. Effect of composition, environmental factors and cement-lime mortar coating on concrete carbonation. Materials and Structures 1992; 25: 293-304.

[22] Steffens A, Dinkler D, Ahrens H. Modeling carbonation for corrosion risk prediction of concrete structures. Cement and Concrete Research 2002; 32: 935-941.

[23] Tang L, Lars-Olof N, Muhammed Basheer PA. Resistance of concrete to chloride ingress: testing and modeling. Published by Spon Press, New York, 2012.

[24] Berke NS, Hicks MC. Predicting chloride profiles in concrete. Corrosion 1994; 50: 234-239.

[25] Browne RD. Mechanism of corrosion of steel in concrete in relation to design, inspection, and repair of offshore and coastal structures, Performance of Concrete in Marine Environment, Detroit, ACI SP 65 (1980) 169-204.

[26] Angst U, Elsener B, Larsen CK. Oystein Vennesland, Critical chloride content in reinforced concrete-A review. Cement and Concrete Research 2009; 39: 1122-1138.

[27] Ann KY, Song HW. Chloride threshold level for corrosion of steel in concrete. Corrosion Science 2007; 49: 4113-4133.

[28] Ann KY, Ahn JH, Ryou JS. The importance of chloride content at the concrete surface in assessing the time to corrosion of steel in concrete structures. Construction and Building Materials 2009; 23: 239-245.

[29] Poupard O, Ait-Mokhtar A, Dumargue P. Corrosion by chlorides in reinforced concrete: determination of chloride concentration threshold by impedance spectroscopy. Cement and Concrete Research 2004; 34: 991-1000.

[30] Yu H, Shi X, Hartt WH, Lu B. Laboratory investigation of reinforcement corrosion initiation and chloride threshold content for self-compacting concrete. Cement and Concrete Research 2010; 40: 1507-1516.

[31] ASTM C 876 Standard Test Method for Half-cell potential of reinforcing steel in concrete, American Society for Testing and Materials, Philadelphia, 1980.

[32] Kelly RG, Scully JR, Shoesmith DW, Buchhei RG. Electrochemical techniques in corrosion science and engineering. Marcel Dekker, New York, 2003.

[33] Jamil HE, Shriri A, Boulif R, Montemor MF, Ferreira MGS. Corrosion behavior of reinforcing steel exposed to an amino alcohol based corrosion inhibitor. Cement and Concrete Composites 2005; 27(6):671-8.

[34] Joiret S, Keddam M, Novoa XR, Perez MC, Rangel C, Takenouti H. Use of EIS, ring-disk electrode, EQCM and Raman spectroscopy to study the film of oxides formed on iron in 1M NaOH. Cement & Concrete Composites 2002; 24(1):7-15.

[35] Behzadnasab M, Mirabedini SM, Kabiri K, Jamali S. Corrosion performance of epoxy coatings containing silane treated ZrO_2 nanoparticles on mild steel in 3.5% NaCl solution. Corrosion Science 2011; 53(1):89-98.

[36] Jegdic BV, Bajat JB, Popic JP, Stevanovic SJ, Miskovic-Stankovic VB. The EIS investigation of powder polymer coatings on phosphate low carbon steel: The effect of $NaNO_2$ in the phosphating bath. Corrosion Science 2011; 53(9):2872-80.

[37] Rudd AL, Breslin CB, Mansfeld F. The corrosion protection afforded by rare earth conversion coatings applied to magnesium. Corrosion Science 2000; 42(2):275-88.

[38] Maitra MG, Sinha M, Mukhopadhyay AK, Middya TR, De U, Tarafdar S. Ion-conductivity and Yong's modulus of the polymer electrolyte PEO-ammonium perchlorate, Solid State Ionics 2007; 178: 167-171.

[39] Zhang Y, Huang Y, Wang L. Study of EVOH based single ion polymer electrolyte: Composition and microstructure effects on the proton conductivity, Solid State Ionics 2006; 177: 65-71.

[40] Rodiguez Presa MJ, Tucceri RI, Florit MI, and Posada D. Constant phase element behavior in the poly (o-toluidine) impedance response. Journal of Electroanalytical Chemistry 2001; 502: 82-90.

[41] Yao Z, Jiang Z, Wang F. Study on corrosion resistance and roughness of micro-plasma oxidation ceramic coatings on Ti alloy by EIS technique. Electrochimica Acta 2007; 52: 4539-4546.

[42] Clear KC, Virmani YP. Corrosion of non-specification epoxy coated rebars in salty concrete, Corrosion 83 1983, NACE, Houston, Paper No. 114, 1983.

[43] Darwin AB, Scantlebury JD. Retarding of corrosion processes on reinforcement bar in concrete with an FBE coating. Cement and Concrete Composite 2002; 24(1): 73-78.

[44] Clear KC. Effectiveness of epoxy-coated reinforcing steel. Concrete International 1992; 5: 58-62.

[45] Sagüé A, Lee J, Chang X, Pickering H, Nystrom E, Carpenter W, Kranc S, Simmons T, Boucher B, and Hierholzer S. Corrosion of Epoxy Coated Rebar in Florida Bridges, *Final Report WPI No. 0510603.* Florida Department of Transportation. 1994.

[46] Zin IM, Lyon SB, Hussain A. Under-film corrosion of epoxy-coated galvanized steel: an EIS and SVET study of the effect of inhibition at defects. Progress in Organic Coatings 2005; 52(2): 126-135.

[47] Bellezze T, Malavolta M, Quaranta A, Ruffini N, Roventi G. Corrosion behaviour in concrete of three differently galvanized steel bars. Cement and Concrete Composites 2006; 28: 246-255.

[48] Tirrarelli F, Bellezze T. Investigation of the major reduction reaction occurring during the passivation of galvanized steel rebars. Corrosion Science 2010; 52(3): 978-983.

[49] Tan ZQ, Hansson CM. Effect of surface condition on the initial corrosion of galvanized reinforcing steel embedded in concrete. Corrosion Science 2008; 50 : 2512-2522.

PAPER

I. MICROSTRUCTURE AND CORROSION RESISTANCE OF ENAMEL COATINGS APPLIED TO SMOOTH REINFORCING STEEL

Fujian Tang[*], Genda Chen[**], Jeffery S. Volz[**], Richard K. Brow[*], and Mike Koenigstein[***]

* Department of Materials Science and Engineering, Missouri University of Science and Technology, Rolla, MO 65401

**Department of Civil, Architectural, and Environmental Engineering, Missouri University of Science and Technology, Rolla, MO 65409-0030

*** Pro-Perma Engineered Coatings, Hypoint, Rolla, MO 65401

ABSTRACT

Corrosion behavior of enamel-coated reinforcing steel bars in 3.5 wt.% NaCl solution is evaluated by open–circuit potential, electrochemical impedance spectroscopy (EIS) and potentiodynamic polarization testing. Three types of enamel coating are investigated: a pure enamel coating, a mixed enamel coating that consists of 50% pure enamel and 50% calcium silicate by weight, and a double enamel coating that has an inner pure enamel layer and an outer 50/50 enamel layer. The coatings are characterized with X-ray diffraction (XRD), scanning electron microscopy (SEM), and energy dispersive X-ray spectroscopy (EDS) techniques. SEM images reveal that all three enamel coatings have a porous structure. The pores in the pure and double enamel are disconnected, while those in the mixed enamel are interconnected. Electrochemical tests demonstrate that both pure and double enamel coatings can significantly improve corrosion resistance, while the mixed enamel coating offers very little protection.

Keywords: Corrosion resistance*;* Enamel coating; EIS; SEM/EDS; XRD.

1. INTRODUCTION

Reinforced concrete is the dominant building material around the world since raw materials such as gravel, sand, water and cement are widely available. In addition, reinforced concrete is often the most economical choice compared to other construction materials. However, due to the inherent permeability of concrete, aggressive species such as chloride ions and carbon dioxide can penetrate the concrete cover and break down the protective passive film formed on the surface of reinforcing steel [1-3]. The breakdown of this passive film initiates corrosion of the reinforcing steel, which in turn causes cracking of the concrete due to expansion of the corrosion products over time. This corrosion-induced cracking of the concrete allows additional moisture to reach the reinforcing steel and thus increase the corrosion rate, eventually leading to severe structural deterioration and reduced load-carrying capacity [4-6].

Existing methods developed to prevent corrosion of steel reinforcement include low-permeability concrete, protective coatings on the reinforcement [7, 8], addition of corrosion inhibitors to the concrete [9, 10], and cathodic protection [11]. Among these methods, protective coatings, which establish a barrier between the porous concrete and reinforcing steel and include fusion-bonded epoxy and zinc (galvanized rebar), are perhaps the most economical and durable methods available. However, none of the existing coatings can provide complete protection, particularly after they suffer minor damage during transportation and/or construction [12, 13]. Ceramic coatings possess excellent chemical resistance and stability at high temperatures and are widely used in industry and on household cooking appliances to protect steel [14]. The ability of ceramic coatings to protect household appliances from corrosion has been investigated and well

documented by previous researchers [15, 16]. In recent years, enamel coatings have been applied to reinforcing steel for corrosion protection and bond enhancement with concrete [17-19].

This study aims at investigating the corrosion performance of enamel-coated reinforcing steel in 3.5 wt.% NaCl solution. Three types of enamel coating are considered in this study: a pure enamel coating, a mixed enamel coating that consists of 50% pure enamel and 50% calcium silicate by weight, and a double enamel coating that has an inner pure enamel layer and an outer 50/50 enamel layer. The coatings are characterized with X-ray diffraction (XRD) and scanning electron microscopy coupled to an energy dispersive spectrometer (SEM/EDS). The corrosion performance of the coatings is evaluated by open-circuit potential, electrochemical impedance spectroscopy and potentiodynamic polarization testing.

2. EXPERIMENTAL DESIGN AND PLAN

2.1 Preparation of Enamel Coatings and Samples

Grade 60 smooth reinforcing steel bar with a diameter of 13 mm was used in this study. Its chemical composition is shown in Table 1. Three types of enamel coatings were used: pure enamel (PE), mixed enamel (ME), and double enamel (DE). The typical chemical composition of the pure enamel is shown in Table 2 [20]. The mixed enamel consisted of 50% pure enamel and 50% calcium silicate by weight that was obtained by mixing enameling frit with Portland cement [21]. The double enamel is a two-layer system with an inner pure enamel layer and an outer mixed enamel layer. For the pure enamel and mixed enamel coatings, after each steel bar was cleansed with a water-based solvent, it was dipped into the appropriate slurry, and then heated for 2 minutes at 150 °C

to drive off moisture. The enamel coated steel bar was then heated in a gas-fired furnace to 810 °C for 10 minutes, and finally cooled to room temperature. For the double enamel coating, cleaned steel bar was first dipped into the pure enamel slurry and heated for 2 minutes at 150 °C, and then dipped into the 50/50 enamel slurry and heated again to drive off moisture before firing to 810 °C for 10 minutes. The final firing treatment melts the glass frit and fuses the enamel to the steel.

Each steel bar sample was sectioned into 89 mm lengths and a copper wire was welded at one end to provide an electrical connection. PVC tubes containing epoxy resin were used to cover the two exposed ends, as shown in Fig.1. Therefore, the actual length of steel potentially exposed to the corrosive environment was approximately 50.8 mm long, and the surface area is approximately 20.26 cm^2. The samples ready for testing are shown in Fig. 2. Three samples were prepared for each condition, including three uncoated steel bars (UN).

2.2 Characterization of Enamel Coatings

The phase composition and microstructure of the enamel coatings were investigated with X-ray diffraction (XRD, Philip X' Pert) and scanning electron microscopy (SEM, Hitachi S4700) coupled to an energy dispersive X-ray spectroscopy (EDS). XRD was conducted directly on the surface of the enamel coated steel bar samples and uncoated steel bar samples. For SEM measurements, 3.0-cm-long longitudinal cross sections were cut, cold-mounted and ground with silicon carbide papers with grits of 80, 180, 320, 600, 800, and 1200. The samples were rinsed with deionized water, cleansed with acetone, and finally dried in air at room temperature. To

avoid any potential disturbance of other elements, a carbon coating was applied during the SEM preparation.

2.3 Electrochemical Tests

All samples were immersed to 3.5 wt. % NaCl solution. The solution was made by mixing purified sodium chloride with deionized water. The pH of the solution was 5.72 at room temperature. A typical three-electrode set-up was used for all electrochemical tests. A 25.4 mm×25.4 mm×0.254 mm platinum sheet functions as a counter electrode, a saturated calomel electrode (SCE) as a reference electrode, and the rebar sample as the working electrode. All three electrodes were connected to a Gamry, Reference 600 potentiostat/galvanostat/ZRA for data acquisition. Open-circuit potentials were recorded for a period of one hour immediately after the samples were immersed in the solution. The electrochemical impedance spectroscopy (EIS) tests were conducted at five points per decade around the open-circuit potential E_{ocp} with a sinusoidal potential wave of 10 mV in amplitude and frequency ranging from 100 kHz to 0.005 Hz. After the EIS tests, the same samples were tested with the potentiodynamic polarization method from E_{ocp}-300 mV to E_{ocp}+1500 mV with a scanning rate of 1.0 mV/s.

3. RESULTS AND DISCUSSION

3.1 Phase Composition of Enamel Coatings Prior to Corrosion Tests

The phase compositions of the uncoated steel bar sample and three enamel-coated samples are shown in Fig. 3. Pure iron (Fe) taken from the uncoated steel samples was analyzed and no rust was detected. The pure enamel coating mainly consists of quartz SiO_2. Crystalline Ca-silicate and mullite phase were detected in both the mixed enamel

and double enamel coatings, most likely from the Portland cement that was added to the enamel slurry to produce the ME coating.

3.2 Microstructures of Enamel Coatings

Fig. 4 shows longitudinal cross sectional SEM images and the elemental analysis of the three types of enamel coatings. As shown in Fig. 4(a), the pure enamel coating is approximately 150 μm thick. It is thinner than both the mixed enamel and double enamel coatings as indicated in Figs. 4(b-1, c-1). The pure enamel coating has air bubbles that were formed during the firing process as a normal part of the enameling process. Its main elements are oxygen (O) and silicon (Si), which is consistent with the XRD results presented in Fig. 3(b). The mixed enamel coating is 300 μm thick, and has an amorphous structure as shown in Fig. 4(b). Based on the elemental analysis, the white phase in the SEM image is calcium silicate and the black phase is mainly the mounting epoxy. The mixed enamel coating has a porous microstructure with interconnected pores, as clearly evidenced by penetration of the mounting epoxy through the coating thickness. Two layers of the double enamel coating with a total thickness of approximately 240 μm can be observed from Fig. 4(c). The inner layer has numerous small pores and a few large pores with a diameter of over 120 μm, which is similar to the pure enamel coating in Fig. 4(a) based on the elemental analysis. The close-up view of the outer layer of the double enamel coating is presented in Fig. 4(d). Two phases can be seen in the SEM image of the outer layer. Based on the elemental analysis, the black phase is similar to the PE coating and the white phase is mainly calcium silicate particles (Figure d-3) from the Portland cement.

3.3 Open-circuit Potential

Fig. 5 shows the change in open-circuit potential up to 3600 sec after the uncoated and three types of enamel-coated steel bars were completely immersed in 3.5 wt.% NaCl solution. The open-circuit potential of all samples decreased rapidly in the first 500 sec and then slowly and linearly to the end of the test. The variation in open-circuit potential among the three identical uncoated samples is significantly more than that of the enamel coated samples. For each type of enamel coating, the final open-circuit potentials of three identical samples are very consistent. The variation between the three types of enamel coating is also very small. At the end of tests after 3600 sec of immersion, the average open-circuit potentials become -641±11.9 mV for the uncoated, -600±0.60 mV for the pure enamel coated, -587±0.70 mV for the mixed enamel coated, and -583±3.10 mV for the double enamel coated samples, respectively. According to ASTM C876, if the potential becomes more negative than -273 mV/SCE, there is a 90% probability of corrosion [22]. As seen from these results, the potential of all samples became more negative than -273 mV/SCE at the time of immersion. This is attributed to pore channels present in the coatings. Through any pathway of pore channels, corrosion immediately started in the exposed steel.

3.4 Electrochemical Impedance Spectroscopy

Fig. 6 presents EIS diagrams of the uncoated and enamel coated steel bars in 3.5 wt.% NaCl solution. Individual points and solid lines represent the experimental data and curve fitting using an equivalent electrical circuit (EEC) model, respectively. As observed from the phase angle-frequency plots, one time constant appeared for uncoated steel bars, and two time constants appeared for enamel coated steel bars although the time

constant at high frequency is not apparent for pure enamel and double enamel coated steel bars. For uncoated steel bars, the time constant is attributed to the interfacial properties between the solution and the substrate steel where corrosion occurs, representing the double layer capacitance and charge transfer resistance. For steel bars coated with enamels, the first time constant in the high frequency range is associated with the dielectric properties of enamel coating, and the second time constant in the low frequency range is attributed to the corrosion properties.

The two equivalent electrical circuit (EEC) models used to fit the test results are illustrated in Fig. 7. Model (a) and Model (b) were used to simulate the uncoated and enamel coated steel bars, respectively. These models were commonly used by other researchers to evaluate the corrosion resistance of steel samples with and without coatings [23-27]. Specifically, R_s represents the solution resistance, CPE_{dl} represents double layer capacitance, R_{ct} represents charge transfer resistance, R_c represents coating resistance, and CPE_c represents coating capacitance. Replacement of capacitance with constant phase element CPE in the EEC models is attributed to the non-homogeneity in the corrosion system [28-29]. The impedance of CPE can be represented by the following equation:

$$Z_{CPE} = 1 \Big/ \left[Y (j\omega)^n \right] \tag{1}$$

Where Y and n are two parameters related to the CPE. When n = 1, CPE resembles a capacitor with capacitance Y. When n =0, CPE represents a resistor with resistance Y^{-1}. The effective capacitance based on CPE parameters was calculated according to the following equation in normal distribution condition [30]:

$$C = Y^{1/n} R^{(1-n)/n} \quad (2)$$

Where parameters $R_{c,}$ Y_c and n_c were used to calculate the effective capacitance of enamel coatings C_c; $R_{ct,}$ Y_{dl} and n_{dl} were used to calculate the effective capacitance of double layer C_{dl}, respectively. The curve-fitting parameters of the EEC model for all samples are tabulated in Table 3, in which Y_c and n_c are related to CPE_c, and Y_{ct} and n_{dl} are related to CPE_{dl}. These parameters were normalized by the exposed surface area of 20.26 cm^2.

Fig.8 shows a comparison of corrosion parameters extracted from the EEC models in terms of the solution resistance R_s, charge transfer resistance R_{ct} and effective double layer capacitance C_{dl}. Each bar represents the average of three samples with an error bar representing one standard deviation. Solution resistance is related to the conductivity of test solution and the microstructure of enamel coatings. The mixed enamel coating has almost the same solution resistance as the uncoated steel bar samples, which is attributed to the interconnected pores inside the mixed enamel coating. These connected pores established numerous pathways for the solution to penetrate (moisture pick-up). However, the pure and double enamel coatings have isolated pores that make it difficult for the solution to go through the coatings. Therefore, the pure enamel and double enamel coatings have a higher solution resistance than the mixed enamel and uncoated samples. Charge transfer resistance measures the ease of electron transfer across the metal surface, which is inversely proportional to corrosion rate [31]. Double layer capacitance also reflects this point. The higher the double layer capacitance, the lower the charge transfer resistance. As indicated in Fig.8, the double enamel coated samples have the highest charge transfer resistance and the lowest double layer capacitance among all three enamel coatings, which indicates the best corrosion performance. The mixed

enamel coating has the lowest charge transfer resistance and the highest double layer capacitance among three coatings, indicating the worst corrosion resistance.

Fig.9 shows the dielectric properties of enamel coatings in terms of coating resistance R_c and coating capacitance C_c. In general, the coating resistance and coating capacitance represent a degree of ability of coating to resist the penetration of electrolyte solution and the diffusion of test solution into the coating, respectively [32]. It is closely related to the dielectric properties, microstructure, thickness, and defect of enamel coatings. As shown in Fig. 9, the double enamel coating has the highest resistance and the lowest capacitance, while the mixed enamel coating has the lowest coating resistance and the highest coating capacitance. The difference is mainly caused by the microstructure of these two coatings, considering similar materials and thicknesses. This further verifies the poor barrier property of the mixed enamel coating. The difference of coating dielectric properties between the pure enamel coating and double enamel coating is mainly attributed to the different coating thickness.

The corrosion resistance of all the tested samples can be ranked in increasing order as uncoated steel bars, mixed enamel coated steel bars, pure enamel coated steel bars, and double enamel coated steel bars. All three types of enamel coating can be used to delay the process of corrosion. The double enamel coating has the best performance in protecting the steel bars from corrosion. Although the mixed enamel coating (~300 μm thick) is approximately twice as thick as the pure enamel coating (~150 μm thick), it still provides less protection of the steel bars against corrosion due to its significantly more porous microstructure as discussed previously. The main reason why the double enamel

coating (240 μm thick) outperforms the pure enamel coating is because the former is thicker than the latter.

3.5 Potentiodynamic Polarization

Potentiodynamic polarization curves of the uncoated and enamel coated samples in 3.5 wt. % NaCl solution are presented in Fig. 10. The current density was calculated by dividing the measured current by the exposed surface area of 20.26 cm^2. The corrosion potential E_{corr} and the corrosion current density i_{corr} of the uncoated samples are smaller and larger than those of the enamel coated samples, respectively. As seen from Fig. 10, the anodic portion of polarization curves was likely influenced by the presence of corrosion products or rust that formed on the surface of uncoated steel bars, affecting the diffusion of oxygen, and resulting in a somewhat passive-like behavior. For coated steel bars, the rust may have filled the holidays of the coating and reduced the corrosion process by affecting the diffusion of oxygen.

The passive current density, i_{pas}, is an important parameter to measure the corrosion resistance of the steel samples in the passive state. A low passive current density indicates a high corrosion resistance. The passive current density obtained from the potentiodynamic polarization curves at a specific potential within the passive zone for all samples are shown in Fig. 11(a). The potential value corresponding to the passive current density is: 0.0 V/SCE for uncoated steel bars; 0.5 V/SCE for pure enamel, mixed enamel and double enamel coated steel bars. The passive current density of uncoated steel bars is higher than the enamel coated steel bars, indicating good protection of enamel coatings in the passive state. Among the three enamel coatings, the double enamel has the lowest passive current density and the mixed enamel coating has the

highest passive current density. This is related to their microstructures. The double enamel coating is less porous than the mixed enamel coating as discussed before. The corrosion product would fill in the connected pores, resulting in a reduction of oxygen available, and reducing the corrosion current density.

The corrosion potential obtained from a potentiodynamic polarization test is shown in Fig. 11(b). All corrosion potentials are lower than the open-circuit potential at the beginning of tests as displayed in Fig. 5. This is mainly caused by the disturbance of the charging current, and the difference between these two potentials would be enhanced with the increase of the scan rate as discussed in [33]. In this study, a scan rate of 1 mV/second was used. However, this effect is small compared to the electrochemical systems of different samples in this study.

The corrosion current density obtained from the polarization curves is shown in Fig. 11 (c). Among the three coating systems, the pure and double enamels reveal a lower corrosion rate than the mixed enamel coating. On the other hand, the mixed enamel coating slightly reduces the corrosion rate compared with the uncoated samples. Overall, these comparisons are consistent with those observed from the EIS testing.

4. CONCLUSIONS

The three types of enamel coatings tested in this study have different microstructures. The pure enamel coating (~150 μm thick) can be characterized by a few small cavities that are disconnected and isolated. The mixed enamel coating (~300 μm thick) has an amorphous structure with an interconnected pore system. The double enamel coating (~240 μm thick) has two distinct layers: the inner pure enamel layer with relatively large pores and the outer mixed enamel layer with scattered calcium silicate

particles. Electrochemical results from open-circuit potential, electrochemical impedance spectroscopy and potentiodynamic polarization demonstrated that all three enamel coatings can enhance the corrosion performance of reinforcing steel bars, and the pure and double enamel coatings consistently outperform the 50/50 enamel coating. The electrochemical results are consistent with the microstructures of the enamel coatings.

ACKNOWLEDGEMENT

The authors gratefully acknowledge the financial support provided by the U.S. National Science Foundation under Award No. CMMI-0900159. The enamel-coated specimens tested in this study were prepared by Pro-Perma Engineered Coatings, Rolla, Missouri.

REFERENCES

[1] Ghods P, Isgor OB, McRae G, Miller T. The effect of concrete pore solution composition on the quality of passive oxide films on black steel reinforcement. Cem & Concre Compost 2009; 31(1): 2-11.

[2] Glass GK, Reddy B, Buenfeld NR. The participation of bound chloride in passive film breakdown on steel in concrete. Corros Sci 2000; 42(11):2013-21.

[3] Ann KY, Song HW. Chloride threshold level for corrosion of steel in concrete. Corros Sci 2007; 49(11):4113-33.

[4] Melchers RE, Li CQ, Lawanwisut W. Probabilistic modeling of structural deterioration of reinforced concrete beams under saline environment corrosion. Struct Saf 2008; 30(5):447-60.

[5] Vidal T, Castel A, Francois R. Corrosion process and structural performance of a 17 year old reinforced concrete beam stored in chloride environment. Cem Concre Res 2007; 37(11):1551-61.

[6] Zhang R, Castel A, Francois R. Concrete cover cracking with reinforcement corrosion of RC beam during chloride-induced corrosion process. Cem Concre Res 2010; 40(3):415-25.

[7] Erdogdu S, Bremner TW, Kondratova IL. Accelerated testing of plain and epoxy-coated reinforcement in simulated seawater and chloride solutions. Cem Concre Res 2001; 31(6):861-7.

[8] Bellezze T, Malavolta M, Quaranta A, Ruffini N, Roventi G. Corrosion behavior in concrete of three differently galvanized steel bars. Cem & Concre Compost 2006; 28(3):246-55.

[9] Saricimen H, Mohammad M, Quddus A, Shameem M, Barry MS. Effectiveness of concrete inhibitors in retarding rebar corrosion. Cem & Concre Compost 2002; 24(1):89-100.

[10] Soylev TA, Richardson MG. Corrosion inhibitors for steel in concrete: State-of-the-art report. Constr Build Mater 2008; 22 (4):609-22.

[11] Parthiban GT, Parthiban T, Ravi R, Saraswathy V, Palaniswamy N, Sivan V. Cathodic protection of steel in concrete using magnesium alloy anode. Corros Sci 2008; 50(12):3329-35.

[12] Manning DG. Corrosion performance of epoxy-coated reinforcing steel: North American experience. Constr Build Mater 1996; 10(5):349-65.

[13] Ghosh R, Singh DDN. Kinetics, mechanism and characterization of passive film formed on hot dip galvanized coating exposed in simulated concrete pore solution. Surf Coat Technol 2007; 201(16-17):7346-59.

[14] Jones DA. Principles and prevention of corrosion. 2nd ed. New Jersey: Prentice Hall; 1996.

[15] Conde A, Damborenea JJ. Electrochemical impedance spectroscopy for studying the degradation of enamel coatings. Corros Sci 2002; 44 (7):1555-67.

[16] Conde A, Damborenea J. Monitoring of vitreous enamel degradation by electrochemical noise. Surf Coat Technol 2002;150 (2-3): 212-7.

[17] Hock VF, Morefield SW, Day D, Weiss CA, Malone JPG. The use of vitreous enamel coatings to improve bonding and reduce corrosion in concrete reinforcing steel. NACE. Paper no. 08220, Corrosion 2008.

[18] Hock VF, Morefield SW, Weiss CA, Malone JPG. The use of vitreous enamel coatings to improve bonding and reducing corrosion in concrete reinforcing steel and stay-in-place forms at army installations. Department of Defense Corrosion Conference 2009. August 10-14, 2009. Gaylord National, Washington DC.

[19] Hackler CL, Weiss CA, Malone PG. Reactive porcelain enamel coatings for reinforcing steel to enhance the bond to concrete and reduce corrosion. XXI International Enamellers Congress, China, May 2008.

[20] NRC. International Critical Tables, vol. 2. Washington (DC): McGraw-Hill, National Research Council (NRC); 1927. P116.

[21] ASTM. Standard specification for Portland cement. American Society of Testing Methods (ASTM), C150-07; 2007a.

[22] ASTM. Standard Test Method for Corrosion Potentials of Uncoated Reinforcing Steel in Concrete. American Society of Testing Methods (ASTM), C876-09; 2009.

[23] Jamil HE, Shriri A, Boulif R, Montemor MF, Ferreira MGS. Corrosion behavior of reinforcing steel exposed to an amino alcohol based corrosion inhibitor. Cem Concr Compost 2005; 27(6):671-8.

[24] Joiret S, Keddam M, Novoa XR, Perez MC, Rangel C, Takenouti H. Use of EIS, ring-disk electrode, EQCM and Raman spectroscopy to study the film of oxides formed on iron in 1M NaOH. Cem & Concre Compost 2002; 24(1):7-15.

[25] Behzadnasab M, Mirabedini SM, Kabiri K, Jamali S. Corrosion performance of epoxy coatings containing silane treated ZrO_2 nanoparticles on mild steel in 3.5% NaCl solution. Corros Sci 2011; 53(1):89-98.

[26] Jegdic BV, Bajat JB, Popic JP, Stevanovic SJ, Miskovic-Stankovic VB. The EIS investigation of powder polymer coatings on phosphate low carbon steel: The effect of $NaNO_2$ in the phosphating bath. Corros Sci 2011; 53(9):2872-80.

[27] Rudd AL, Breslin CB, Mansfeld F. The corrosion protection afforded by rare earth conversion coatings applied to magnesium. Corros Sci 2000; 42(2):275-88.

[28] Rodiguez Presa MJ, Tucceri RI, Florit MI, and Posada D. Constant phase element behavior in the poly (o-toluidine) impedance response. J Electroanal Chem 2001; 502 (1-2): 82-90.

[29] Yao Z, Jiang Z, Wang F. Study on corrosion resistance and roughness of micro-plasma oxidation ceramic coatings on Ti alloy by EIS technique. Electrochim Acta 2007; 52 (13): 4539-46.

[30] Hirschorn B, Orazem ME, Tribollet B, Vivier V, Frateur I, Musiani M. Determination of effective capacitance and film thickness from constant-phase-element parameters. Electrochim Acta 2010; 55 (21): 6218-27.

[31] Hassan HH, Abdelghani E, Amin MA. Inhibition of mild steel corrosion in hydrochloric acid solution by triazole derivatives: Part I. Polarization and EIS studies. Electrochim Acta 2007; 52 (22): 6359-66.

[32] Zhang Y, Shao Y, Zhang T, Meng G, Wang F. The effect of epoxy coating containing emeraldine base and hydrofluoric acid doped polyaniline on the corrosion protection of AZ91D magnesium alloy. Corros Sci 2011; 53 (11): 3747-55.

[33] Zhang XL, Jiang ZhH, Yao ZhP, Song Y, Wu ZhD. Effects of scan rate on the potentiodynamic polarization curve obtained to determine the Tafel slopes and corrosion current density. Corros Sci 2009; 51 (3): 581-87.

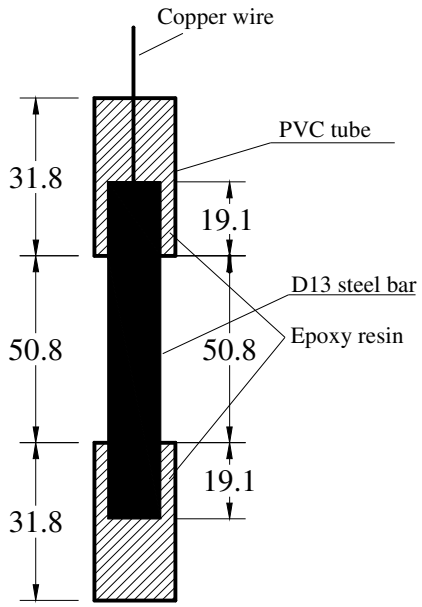

Fig.1. Geometry of rebar samples (unit: mm).

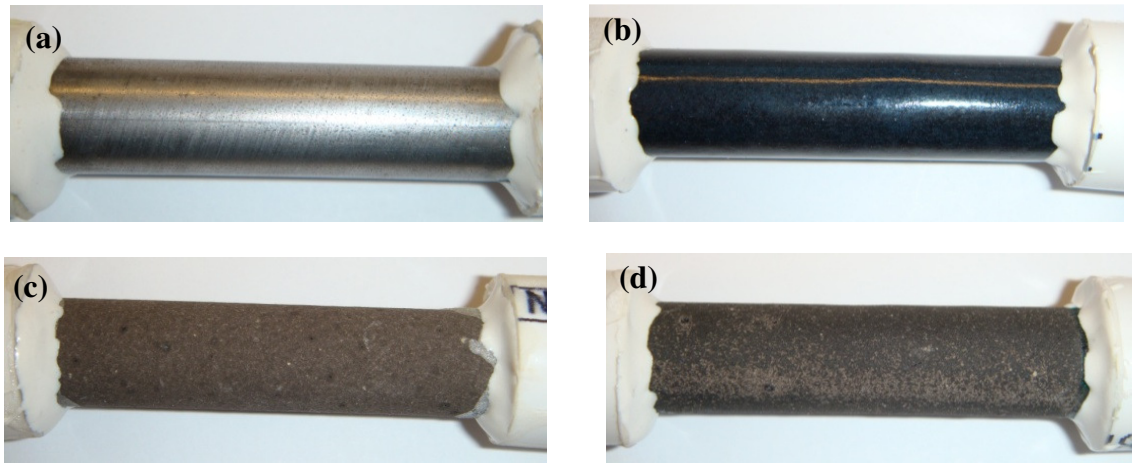

Fig.2. Samples for: (a) uncoated, (b) pure enamel coated, (c) mixed enamel coated, and (d) double enamel coated steel bar.

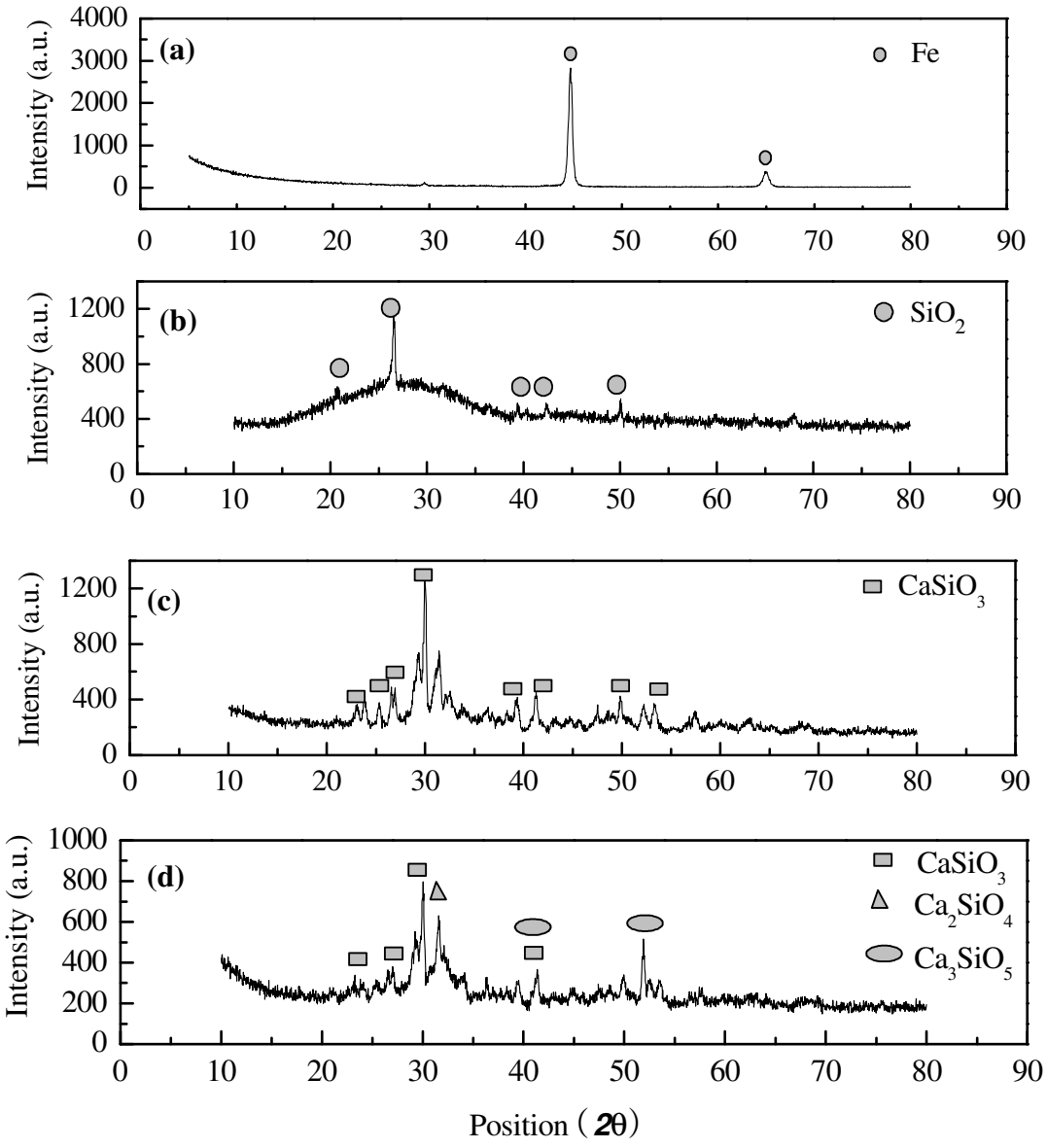

Fig.3. XRD patterns for: (a) uncoated, (b) pure enamel, (c) mixed enamel, and (d) double enamel coatings.

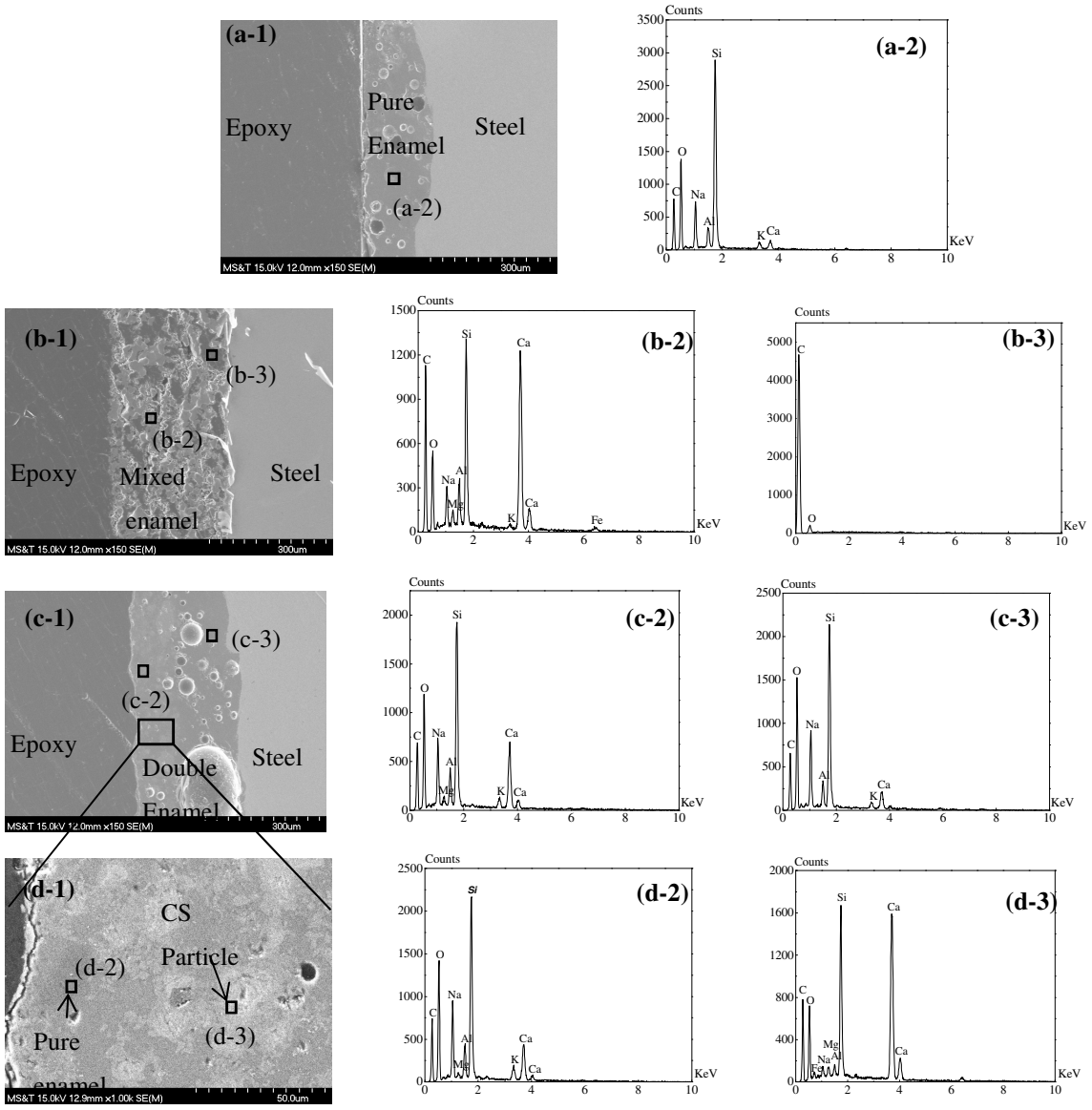

Fig.4. SEM images and elemental analysis for: (a-1) (a-2) pure enamel, (b-1) (b-2) (b-3) mixed enamel, (c-1) (c-2) (c-3) double enamel, and (d-1) (d-2) (d-3) outer layer of the double enamel coatings.

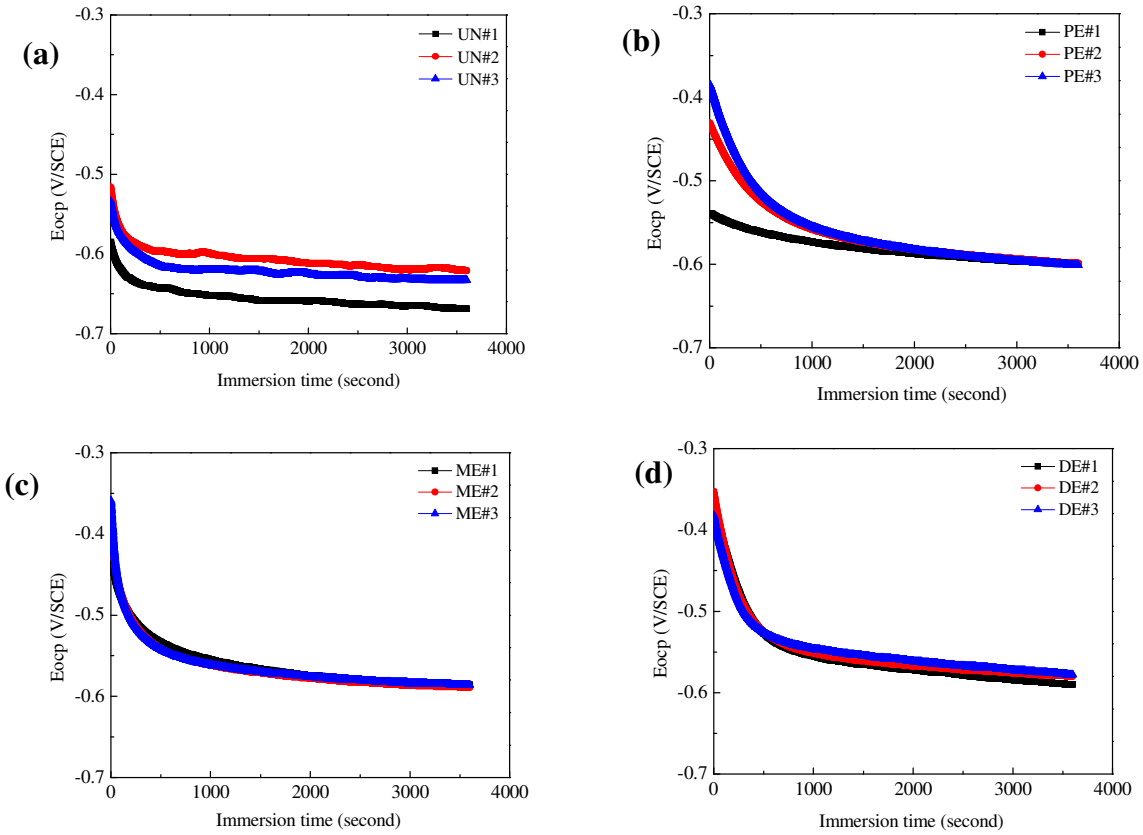

Fig.5. Open-circuit potential evolution with time for: (a) uncoated, (b) pure enamel coated, (c) mixed enamel coated, and (d) double enamel coated steel bars.

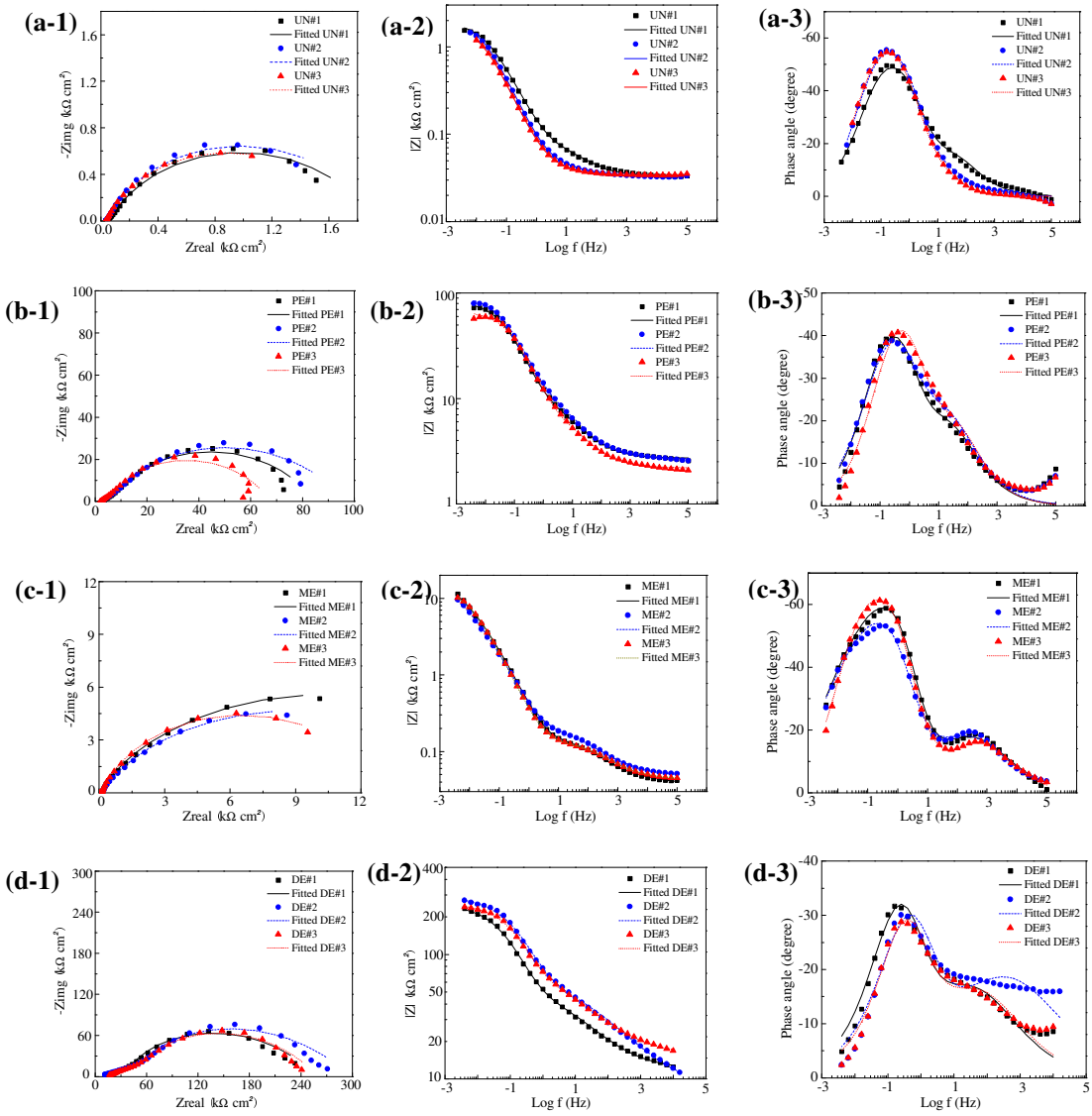

Fig.6. EIS diagrams (number 1: Nyquist plot; number 2 and 3: Bode plots) for: (a) uncoated, (b) pure enamel coated, (c) mixed enamel coated, and (d) double enamel coated steel bars.

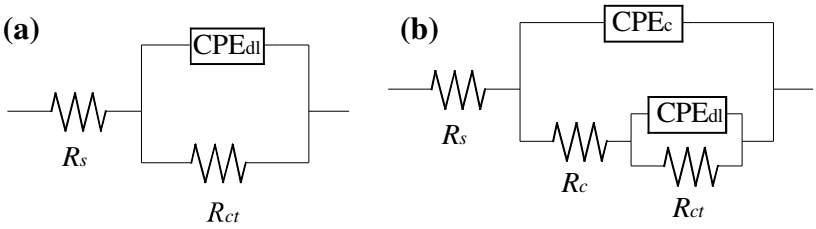

Fig.7. Equivalent electrical circuit models for: (a) uncoated steel bar, and (b) enamel coated steel bar.

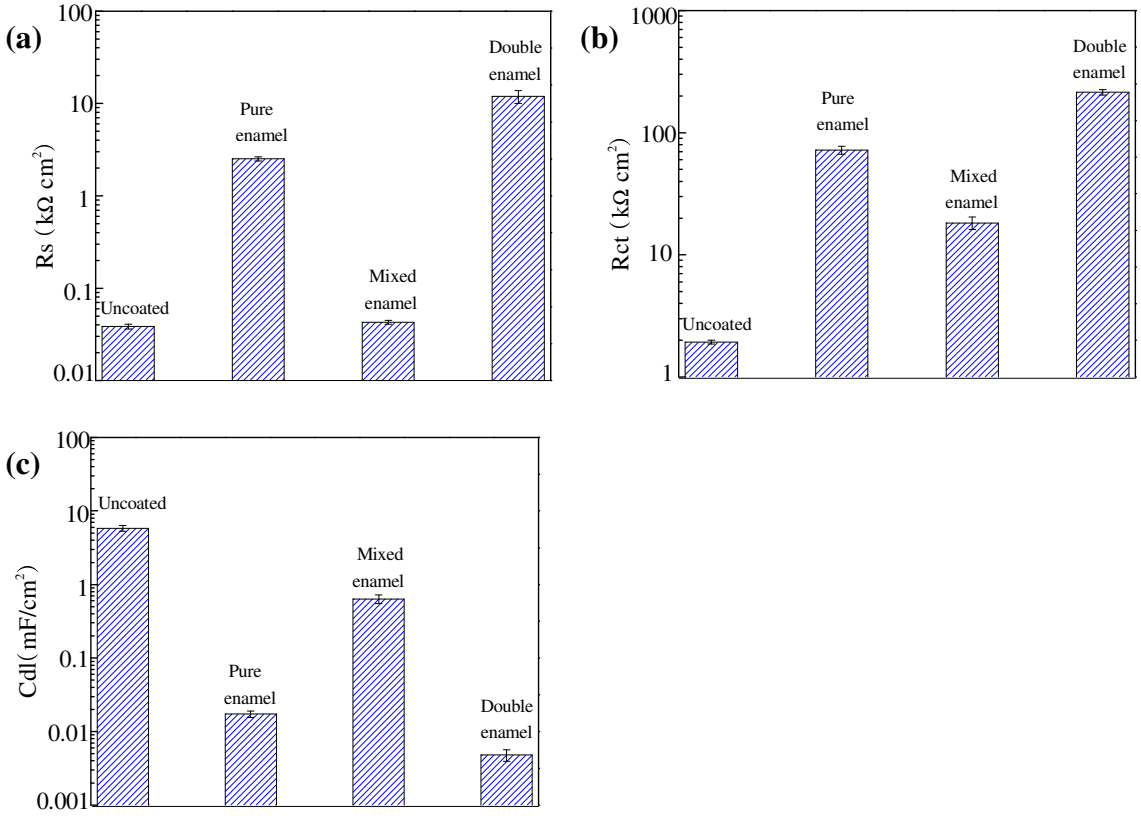

Fig.8. Comparison of corrosion properties: (a) solution resistance R_s, (b) charge transfer resistance R_{ct}, and (d) double layer capacitance C_{dl}.

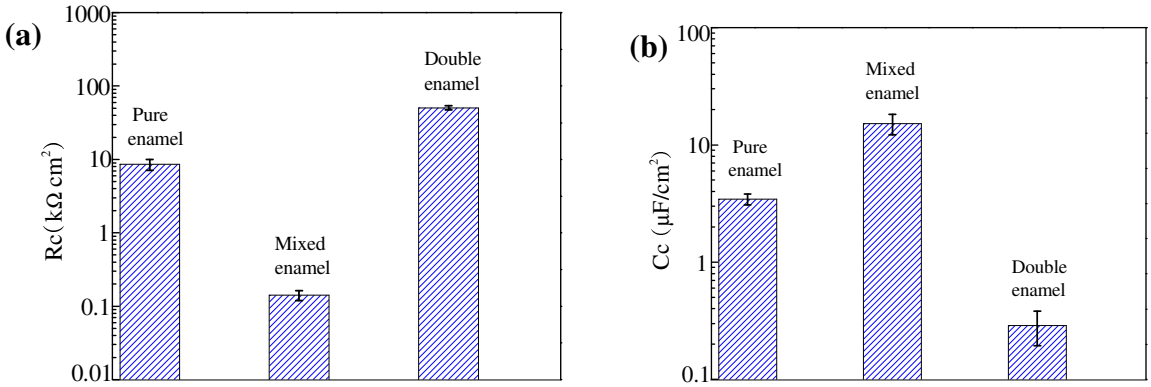

Fig.9. Comparison of dielectric properties of three enamel coatings: (a) coating resistance, and (b) coating capacitance.

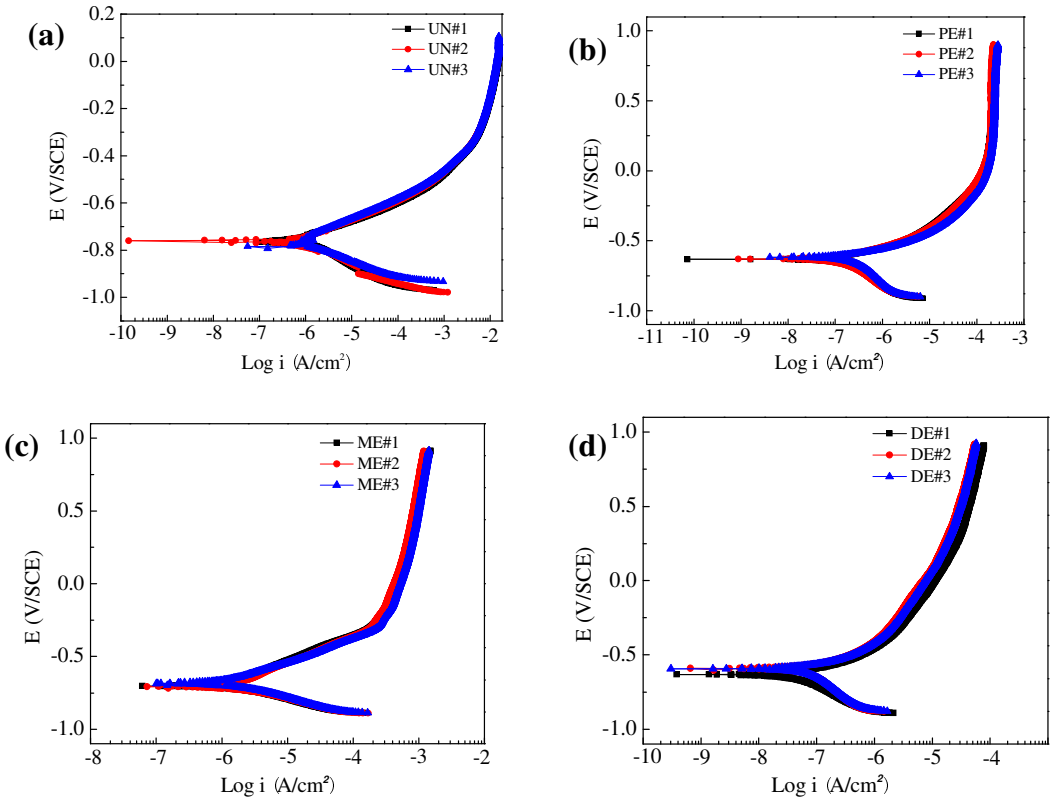

Fig.10. Potentiodynamic polarization curves for: (a) uncoated, (b) pure enamel coated, (c) mixed enamel coated, and (d) double enamel coated steel bars.

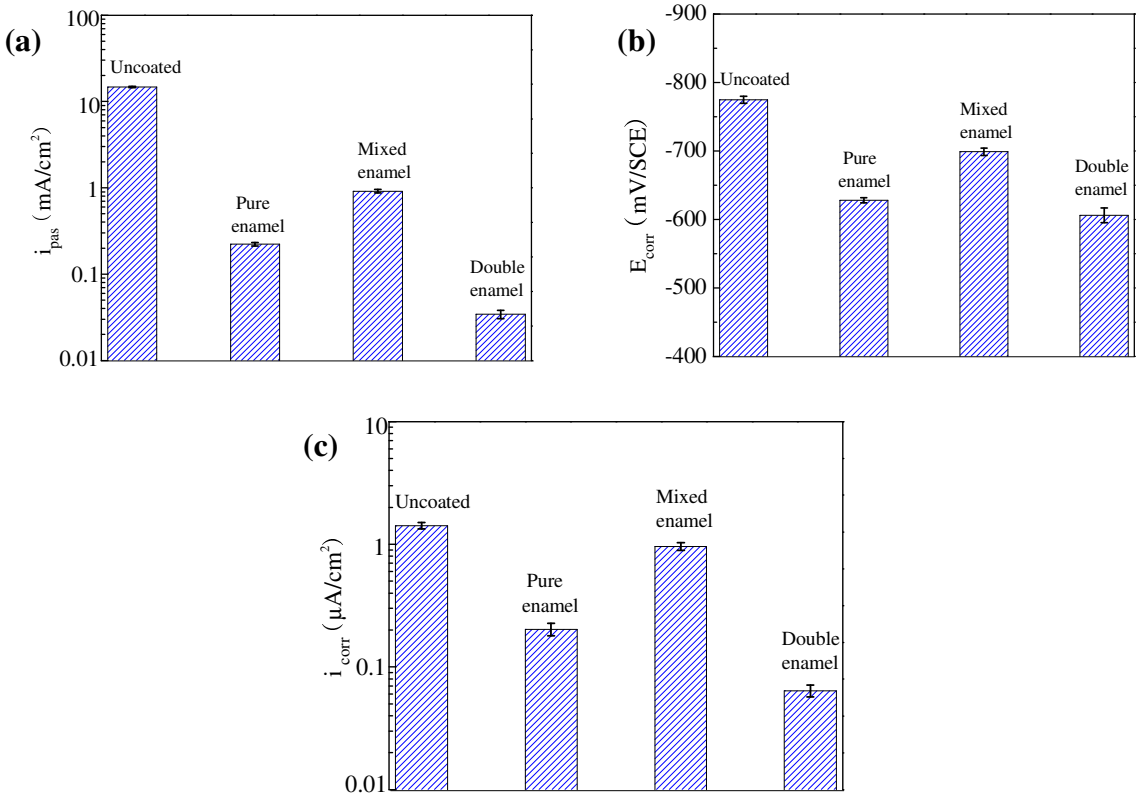

Fig.11. Parameters extracted from potentiodynamic polarization curves: (a) passive current density, (b) corrosion potential, and (c) corrosion current density.

Table 1

Chemical composition of steel bar

Element	C	Si	Mn	P	S	Cr	Mo	Ni	Co	Cu	V	Sn	Fe
Wt.%	0.43	0.22	0.95	0.15	0.07	0.17	0.03	0.10	0.01	0.46	0.02	0.02	97.37

Table 2

Chemical composition of pure enamel

Materials	SiO_2	B_2O_3	Na_2O	K_2O	CaO	CaF_2	Al_2O_3	ZrO_2	CoO	MnO_2	NiO
Wt.%	44.0	19.3	15.8	2.8	0.0	4.7	4.6	5.3	0.9	1.5	1.0

Table 3

EEC parameters obtained by fitting with experimental data

		R_s (Ω cm^2)	Y_c ($\mu F\ cm^{-2}\ s^{-(1-n_c)}$)	n_c	R_c ($k\Omega$ cm^2)	Y_{dl} (($\mu F\ cm^{-2}\ s^{-(1-n_{dl})}$))	n_{dl}	R_{ct} ($k\Omega$ cm^2)
Uncoated	UN#1	44	-	-	-	2230.0	0.67	2.0
	UN#2	36	-	-	-	3110.0	0.74	2.0
	UN#3	35	-	-	-	3690.0	0.75	1.8
Pure enamel coated	PE#1	270	14.7	0.59	7.9	19.3	0.78	74.6
	PE#2	267	15.4	0.57	11.9	14.7	0.77	82.5
	PE#3	219	12.6	0.63	5.9	15.3	0.78	59.5
Mixed enamel coated	ME#1	38	318.0	0.52	0.1	352.0	0.89	22.4
	ME#2	47	326.0	0.50	0.2	412.0	0.83	19.1
	ME#3	43	161.0	0.58	0.1	561.0	0.84	13.3
Double enamel coated	DE#1	11900	3.7	0.48	42.4	6.4	0.80	207.0
	DE#2	8000	2.0	0.42	56.6	3.6	0.77	241.0
	DE#3	15800	2.4	0.48	52.8	4.3	0.81	195.0

II. ELECTROCHEMICAL CHARACTERISTICS OF SAND-PARTICLE MODIFIED ENAMEL CAOTINGS APPLIED TO SMOOTH STEEL BAR BY EIS

Fujian Tang[*], Richard K. Brow[*], Genda Chen[**], and Mike Koenigstein[***]

* Department of Materials Science and Engineering, Missouri University of Science and Technology, Rolla, MO 65401

**Department of Civil, Architectural, and Environmental Engineering, Missouri University of Science and Technology, Rolla, MO 65409-0030

*** Pro-Perma Engineered Coatings, Hypoint, Rolla, MO 65401

ABSTRACT

Corrosion behavior of sand particle modified enamel coating applied to reinforcing steel bars in 3.5 wt.% NaCl solution was evaluated by electrochemical impedance spectroscopy (EIS). Six different percentages of sand particles by weight were investigated: 5%, 10%, 20%, 30%, 50%, and 70%. The surface and cross sectional morphologies of these coatings were characterized with scanning electron microscopy (SEM). The results were compared with samples modified by the addition of calcium silicate, described in a previous study. SEM images revealed that enamel coating wet well with sand particles, and no micro-cracks appeared at the interfaces. Compared with enamel coating modified by calcium silicate, sand particle modified enamel coatings performed better in terms of both coating and corrosion resistances. However, some of the sand particles, which have different coefficients than thermal expansion than the enamel coating, generate weak zones around them, resulting in potential active corrosion. Therefore, quality control of the sand particle is the key factor to improve the corrosion performance when sand is added to the enamel.

Keywords: Corrosion resistance*;* Enamel coating; EIS; SEM.

1. INTRODUCTION

Two of the most commonly used coatings to protect reinforcement steel from corrosion are fusion-bonded epoxy and hot-dipped galvanized zinc [1-3]. However, neither of these two coatings can provide full protection to steel from corrosion. One of the major problems for epoxy-coated rebar is bond degradation between the bar and the concrete [4, 5]. The bond between rebar and concrete is a major factor in reinforced concrete (RC) design and this property relates to the force transmission between the rebar and the concrete. Other problems are coating imperfections and external damage, which would cause disbondment and under-film corrosion [6]. Hot-dip galvanized zinc coatings also have two main concerns when used in engineering applications. First, the zinc coating corrodes vigorously due to the high alkaline environment in fresh concrete if no passive film is formed. Second, the hydrogen produced in the cathodic reaction increases the porosity of adjacent cement pastes and thus reduces the bond strength between the rebar and the concrete [7].

Porcelain enamel, as a coating material for reinforcement steel, has been studied for both enhanced corrosion resistance and enhanced bond strength in concrete in our previous work [8-12]. Specifically, three types of enamel coatings (pure, mixed, and double enamel) applied on reinforcement steel bar were investigated. Enamel coatings modified by calcium silicate (mixed enamel) are made by mixing 50% calcium silicate from Portland cement with 50% pure enamel, which was designed to increase the bond strength between steel bar and concrete by chemical reaction with the surrounding concrete. Results showed that the bond strength increased to different extents, however the corrosion resistance decreases due to changes in the coating microstructure. Pure enamel had isolated air bubbles and could prevent penetration of aggressive chemicals to

the steel. The addition of calcium silicate to the enamel, however, produced connected channels in the enamel which provide pathways for aggressive chemical to reach the steel.

Studies conducted by other researchers have shown that adding sand into an epoxy coating can increase the bond strength with concrete without affecting the corrosion resistance [13, 14]. Therefore, the addition of sand particles into the enamel coating could be a good option for both increased corrosion resistance and enhanced bond strength, because the sand particles can increase the enamel coating surface roughness which would increase the mechanical interlocking with concrete.

This study aims to investigate the corrosion performance of enamel coating modified by sand particles applied to smooth steel bar in 3.5 wt% NaCl solution for a period of 35 days. Sand particles were added to levels by weight between 5% and 70%. The surface and cross-sectional morphologies of these coatings were characterized with scanning electron microscopy. The corrosion performance of the coatings was evaluated by electrochemical impedance spectroscopy. In addition, the results were also compared with those obtained for enamel coatings modified by calcium silicate, reported in earlier studies.

2. EXPERIMENTAL PROCEDURES

2.1 Preparation of Enamel Coatings and Samples

Enamel coatings were deposited from slurries and fused to their substrates at high temperatures. An enamel slurry is made by milling glass frits, clay and certain electrolytes, then mixing with water to provide a stable suspension. In this study, a commercially-available alkali borosilicate glass frit from PEMCO (Product No. PO2025)

was used for the pure enamel. Its chemical composition is given in Table 1 [15]. A slurry of the pure enamel was made by first adding 454 kg of enamel frit to 189.3 litres of water and mixing them for 20 minutes, and then adding clay (31.8 kg) and borax (2.3 kg) as suspension agents, and mixing again for 3.5 hours. To get different sand particle contents, six different percentages of sand particles by weight were added into pure enamel frits including 5%, 10%, 20%, 30%, 50%, and 70%. The sand particles used have a maximum diameter of 1.0 mm.

Grade 60 smooth reinforcing steel bar with a diameter of 13 mm was used in this study. Its chemical composition was determined and is shown in Table 2. Before coating, each steel bar was cleansed with a water-based solvent. For the coating process, the steel bar was dipped into the enamel slurry with different sand particle percentages, and then heated for 2 minutes at 150 °C to drive off moisture. The enamel coated steel bar was then heated in a gas-fired furnace to 810 °C for 10 minutes, and finally cooled to room temperature. The firing treatment at high temperature melts the glass frit and fuses the enamel to the steel.

Each steel bar sample coated with sand particle modified enamel was sectioned into 89 mm lengths and a copper wire was welded at one end to provide an electrical connection. PVC tubes containing epoxy resin were used to cover the two exposed ends, as shown in Fig.1. Therefore, the actual length of steel potentially exposed to the corrosive environment was approximately 50.8 mm long, and the surface area was approximately 20.3 cm^2. The samples ready for testing are shown in Fig. 2, and three samples were prepared for each corrosion condition.

2.2 Characterization of Enamel Coating with Sand Particles

The microstructures of the enamel coatings were investigated with scanning electron microscopy (SEM, Hitachi S4700). Two types of samples were prepared to get both the surface and the cross-sectional morphologies. For the observation of surface morphologies, a 3.0-cm-long sand-particle modified enamel coated steel bar was used. For the observation of cross section, 1.0-cm-long samples were sliced from the bars and these were cold-mounted in epoxy and ground with silicon carbide papers with grits of 80, 180, 320, 600, 800, and 1200. The samples were rinsed with deionized water, cleansed with acetone, and finally dried in air at room temperature. To avoid sample charging, a carbon coating was applied prior to SEM analyses.

2.3 Electrochemical Test

All samples were immersed to 3.5 wt. % NaCl solution. The solution was made by mixing purified sodium chloride with deionized water. The pH of the solution was 5.72 at room temperature. The tests were conducted after 1 day, 7 days, 14 days, 21 days and 35 days in the NaCl solution. A typical three-electrode set-up was used for the EIS tests. A 25.4 mm×25.4 mm×0.254 mm platinum sheet functioned as a counter electrode, a saturated calomel electrode (SCE) as a reference electrode, and the rebar sample as the working electrode. All three electrodes were connected to a Gamry, Reference 600 potentiostat/galvanostat/ZRA for data acquisition. The tests were conducted at five points per decade around the open-circuit potential E_{ocp} with a sinusoidal potential wave of 10 mV in amplitude and frequency ranging from 100 kHz to 0.005 Hz. After 35 days of immersion test, all samples were taken out of the solution for surface visual observation.

3. RESULTS AND DISCUSSION

3.1 Microstructure of Enamel Coating with Sand Particles

Fig. 3 shows the surface and cross-sectional SEM images of the sand particle modified enamel coatings. As shown in Fig. 3(a), the surface is uniform, and all the sand particles were embedded completely in the enamel coatings. However, the surfaces were not smooth, the location at sand particle are much higher than that without sand particles. Figure 3(b) shows the magnified SEM images of sand particles embedded in the enamel coating. No shrinkage-induced micro-cracks were observed around the sand particles. Figure 3(c) shows the comparison of two sand particle modified enamel coatings with 10% and 50%; it can be clearly seen that the sample with 50% sand particles has a much rougher surface than that with 10% sand particles. Figure 3(d) shows the surface morphology with damaged coating area induced in the sample preparation process. Many small air bubbles (50 μm in diameter) distributed uniformly underneath a glassy pure enamel surface. Figures 3(e) and 3(f) show the cross-sectional SEM images and reveal good wetting between the enamel and the sand particles; no micro-cracks were observed at the interface of sand particles and enamel coating. There are some air bubbles distributed in the enamel coating, and they are not accumulated around the sand particles.

3.2 Electrochemical Impedance Spectroscopy

Fig. 4 presents representative EIS diagrams of the sand particle modified enamel coated steel bars in 3.5 wt.% NaCl solution for up to 35 days. As observed from the Nyquist diagrams, one big depressed semi-circle appeared for all samples. After one day of testing, the radii of the semi-circle for the sample with 5% sand particles dropped

significantly. However, for other samples with sand particle percentages from 10% to 70%, the radii of the semi-circle increased over time, and this increase became much greater with an increase in the percentage of sand particles. For example, the 1 day radii of the semi-circle for sample with 5% sand particles is similar to that at the other different days, whereas a significant increase could be observed for samples with 50% and 70% sand particles. In addition, there is also a small semi-circle in the high frequency range of the one-day Nyquist plots.

The equivalent electrical circuit (EEC) method is usually used to fit the EIS test results, and this is illustrated in Fig. 5. This model was commonly used by other researchers to evaluate the corrosion resistance of steel samples with and without coatings [16-19]. Specifically, R_s represents the solution resistance, R_c represents coating resistance, CPE_c represents coating capacitance, CPE_{dl} represents double layer capacitance, and R_{ct} represents charge transfer resistance. Replacement of capacitance with constant phase element CPE in the EEC models is attributed to the non-homogeneity in the corrosion system [20-21]. The impedance of CPE can be represented by the following equation:

$$Z_{CPE} = 1 \Big/ \left[Y (j\omega)^n \right] \tag{1}$$

where Y and n are two parameters related to the CPE. When n = 1, CPE resembles a capacitor with capacitance Y. When n =0, CPE represents a resistor with resistance Y^{-1}. The effective capacitance based on CPE parameters was calculated according to the following equation in normal distribution condition [22]:

$$C = Y^{1/n} R^{(1-n)/n} \quad (2)$$

where parameters $R_{c,}$ Y_c and n_c were used to calculate the effective capacitance of the coatings C_c; $R_{ct,}$ Y_{dl} and n_{dl} were used to calculate the effective capacitance of double layer C_{dl}, respectively. The curve-fitting parameters of the EEC model for all samples are tabulated in Table 3, in which Y_c and n_c are related to CPE_c, and Y_{ct} and n_{dl} are related to CPE_{dl}. These parameters were normalized by the exposed surface area of 20.3 cm^2.

ZSimpWin was used to fit the EIS data with the different EEC models. The chi-squared values in the fitting are in the range from 10^{-4} to 10^{-3}, indicating an acceptible fitting.

Fig.6 shows the dielectric properties of sand particle-modified enamel coatings in terms of coating resistance R_c and coating capacitance C_c. Each bar represents the average of three samples with an error bar representing one standard deviation. In general, the coating resistance and coating capacitance represent a degree of ability of the coating to resist the penetration of the electrolyte solution and the diffusion of test solution into the coating, respectively [24]. It is closely related to the dielectric properties, microstructure, thickness, and defects of the enamel coatings. As shown in Fig. 6, no general trend was observed for coating resistance over time, and the average measured coating resistance is in the range of 3~30 kΩ cm^2 for all samples with different percentages of sand particle. Fig. 6(b) shows the coating capacitance, and all the samples had an increased coating capacitance over time except the sample with 5% sand particle. The increase of coating capacitance is due to the penetration of chloride into the coating layer, increasing its conductivity. The measured coating capacitance has a great scatter compared with coating resistance.

Fig.7 shows the evolution of charge transfer resistance R_{ct} and effective double layer capacitance C_{dl} with time. Charge transfer resistance measures the ease of electron transfer across the metal surface, which is inversely proportional to corrosion rate [23]. Double layer capacitance also reflects this point. As indicated in Fig. 7(a), no general trend was observed over time for charge transfer resistance, and all the samples have a charge transfer resistance in the range of 30~2000 kΩ cm^2. However, there is an increase of double layer capacitance at 7 days for all samples, after which it remains stable with time up to 35 days. The increase of double layer capacitance is probably attributed to the enlargement of active corrosion area.

3.3 Visual Observation

Figure 8 shows the surface conditions of all sand particle modified enamel coated samples after being completely immersed in 3.5 wt.% NaCl solution for 35 days. Most of the corrosion products accumulated around some sand particles, but not around all sand particles.

Figure 9 shows the surface observation of sand particles on the enamel coating before and after corrosion testing. Two consequences of the enamel processing were observed: the first is sand particles surrounded by a weak zone (Fig. 9c), and the second is sand particles without a weak zone (Fig. 9d). Sand particles with a weak zone would be potential corrosion sites. As can be observed in Fig. 9b, all corrosion products surrounded the sand particle. The weak zone is attributed to shrinkage cracks generated during the enamel cooling due to different coefficients of thermal expansion between the enamel body and the sand particles. In order to improve the corrosion resistance of sand particle-modified enamel coating, quality control of the sand particles is very important. All the

sand particles should have the same coefficient of thermal expansion with the enamel coating.

3.4 Comparison with Previous Study

In the previous study [10], smooth rebar samples were tested using the EIS technique with three types of enamel coatings: pure enamel, mixed enamel, and double enamel. Pure enamel is a commercially available product, mixed enamel consisted of 50% pure enamel and 50% calcium silicate by weight, and double enamel had an inner layer of pure enamel and an outer layer of mixed enamel. Figure 10 shows the comparison of coating properties for all nine types of enamel coatings in terms of coating resistance and coating capacitance. The addition of calcium silicate into the pure enamel reduced the coating resistance significantly, whereas the use of sand particles did not affect the coating resistance of pure enamel as indicated in Fig. 10(a). The coating capacitance increased a little due to the addition of calcium silicate for mixed enamel coating. The coating capacitance of sand particle-modified enamel coating increased with the sand particle percentage reached to 20%, then decreased at 30% and 50%. The samples with 70% sand particle had the lowest coating capacitance of 8.4×10^{-11} F/cm^2.

Figure 11 shows the comparison of ten different samples in terms of double layer capacitance and charge transfer resistance. The use of calcium silicate reduced the charger transfer resistance from 72 kΩ cm^2 to 18 kΩ cm^2, while the addition of sand particles increased the charge transfer resistance. When the sand particle addition is 5%, the charger transfer resistance was 700 kΩ cm^2, which is 10 times higher than pure enamel. With an increase in sand particle percentage, the charge transfer resistance decreased. It reached 56 kΩ cm^2 when the sand particle content was 70%, which is a little

lower than pure enamel. This is because the number of sand particles with potential damage zones increases, resulting in a greater number of active corrosion sites. Figure 11(b) shows the double layer capacitance for ten types of samples. Use of calcium silicate increased the double layer capacitance from 1.73×10^{-5} Fm/cm^2 to 6.35×10^{-4} Fm/cm^2, while addition of sand particles did not significantly affect the double layer capacitance.

4. CONCLUSIONS

Steel rebar with enamel coatings modified by different percentages of sand particles were tested in 3.5 wt% NaCl solution by EIS. Enamel coatings with some sand particles can wet the steel very well and no micro-cracks appeared in the composite coatings. Electrochemical results demonstrated that both the coating and corrosion properties of the samples with different percentages of sand particle did not change significantly with corrosion time. Compared with enamel coatings modified by calcium silicate, samples with sand particle performed much better in terms of both coating uniformity and corrosion properties. However, some of the sand particles would have different coefficient of thermal expansion, and generate a damage zone around these sand particles, potentially resulting in active corrosion. Therefore, quality control of the sand particles is the key factor to improve the corrosion performance when added in the enamel coating.

ACKNOWLEDGEMENT

The authors gratefully acknowledge the financial support provided by the U.S. National Science Foundation under Award No. CMMI-0900159. The enamel-coated specimens tested in this study were prepared by Pro-Perma Engineered Coatings, Rolla, Missouri.

REFERENCES

[1] Kobayashi K, Takewaka K. Experimental studies on epoxy coated reinforcing steel for corrosion protection. The International Journal of Cement Composites and Lightweight Concrete 1984; 6(2): 99-116.

[2] Darwin AB, Scantlebury JD. Retarding of corrosion processes on reinforcement bar in concrete with an FBE coating. Cement and Concrete Composites 2002; 24(1): 73-78.

[3] Sistonen E, Cwirzen A, Puttonen J. Corrosion mechanism of hot-dip galvanized reinforcement bar in cracked concrete. Corrosion Science 2008; 50(12): 3416-3428.

[4] Treece RA, Jirsa JO. Bond strength of Epoxy-coated Reinforcing bars. ACI Material Journal 1989; 86(2): 167-174.

[5] Miller GG, Kepler JL, Darwin D. Effect of epoxy coating thickness on bond strength of reinforcing bars. ACI Structural Journal 2003; 100(3): 314-320.

[6] Manning DG. Corrosion performance of epoxy-coated reinforcing steel: North American experience. Construction and Building Materials 1996; 10(5): 349-365.

[7] Tan ZQ, Hansson CM. Effect of surface condition on the initial corrosion of galvanized reinforcing steel embedded in concrete. Corrosion Science 2008; 50: 2512-2522.

[8] Tang F, Chen G, Volz JS, Brow RK, Koenigstein ML. Cement-modified enamel coating for enhanced corrosion resistance of steel reinforcing bars. Cement and Concrete Composites 2013; 35(1): 171-180.

[9] Tang F, Chen G, Brow RK, Volz JS, Koenigstein ML. Corrosion resistance and mechanism of steel rebar coated with three types of enamel. Corrosion Science 2012; 59: 157-168.

[10] Tang F, Chen G, Volz JS, Brow RK, Koenigstein ML. Microstructure and corrosion resistance of enamel coatings applied to smooth reinforcing steel. Construction and Building Materials 2012; 35: 376-384.

[11] Yan D, Reis S, Tao X, Chen G, Brow RK, Koenigstein ML. Effect of chemically reactive enamel coating on bonding strength at steel/mortar interface. Construction and Building Materials 2012; 28(1): 512-518.

[12] Wu C, Chen G, Volz JS, Brow RK, Koenigstein ML. Local bond strength of vitreous enamel coated rebar to concrete. Construction and Building Materials 2012; 35: 428-439.

[13] Chang JJ, Yeih W, Tsai CL. Enhancement of bond strength for epoxy-coated rebar using river sand. Construction and Building Materials 2002; 16(8) 465-472.

[14] Chang JJ, Yeih W, The effect of particle shape on bond strength improvement of epoxy-particle coating composites. J Material Science and Technology 2001; 9(2) 153-160.

[15] NRC. International Critical Tables, vol. 2. Washington (DC): McGraw-Hill, National Research Council (NRC); 1927. P116.

[16] Shi X, Nguyen TA, Suo Z, Liu Y, Avci R. Effect of nanoparticles on the anticorrosion and mechanical properties of epoxy coating. Surface and Coatings Technology 2009; 204: 237-245.

[17] Huang Y, Shi H, Huang H, Daugherty J, Wu S, Ramanathan S, Chang C, Mansfeld F. Evaluation of the corrosion resistance of anodized aluminum 6061 using electrochemical impedance spectroscopy (EIS). Corrosion Science 2008; 3569-3575.

[18] Aperador W, Mejia de Gutierrez R, Bastidas DM. Steel corrosion behavior in carbonated alkali-activated slag concrete. Corrosion Science 2009; 51: 2027-2033.

[19] Choi YS, Kim JG, Lee KM. Corrosion behavior of steel rebar embedded in fly ash concrete. Corrosion Science 2006; 48: 1733-1745.

[20] Rodiguez Presa MJ, Tucceri RI, Florit MI, and Posada D. Constant phase element behavior in the poly (o-toluidine) impedance response. Journal of Electroanalytical Chemistry 2001; 502 (1-2): 82-90.

[21] Yao Z, Jiang Z, Wang F. Study on corrosion resistance and roughness of micro-plasma oxidation ceramic coatings on Ti alloy by EIS technique. Electrochimica Acta 2007; 52 (13): 4539-46.

[22] Hirschorn B, Orazem ME, Tribollet B, Vivier V, Frateur I, Musiani M. Determination of effective capacitance and film thickness from constant-phase-element parameters. Electrochimica Acta 2010; 55 (21): 6218-27.

[23] Hassan HH, Abdelghani E, Amin MA. Inhibition of mild steel corrosion in hydrochloric acid solution by triazole derivatives: Part I. Polarization and EIS studies. Electrochim Acta 2007; 52 (22): 6359-66.

[24] Zhang Y, Shao Y, Zhang T, Meng G, Wang F. The effect of epoxy coating containing emeraldine base and hydrofluoric acid doped polyaniline on the corrosion protection of AZ91D magnesium alloy. Corros Sci 2011; 53 (11): 3747-55.

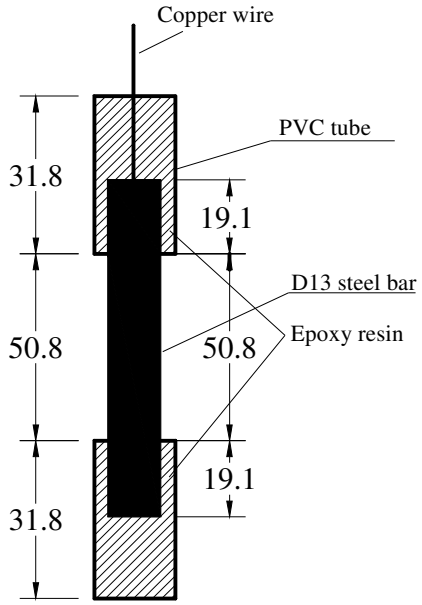

Fig.1. Geometry of rebar samples (unit: mm).

Fig.2. Sand particle-modified enamel coated steel bar.

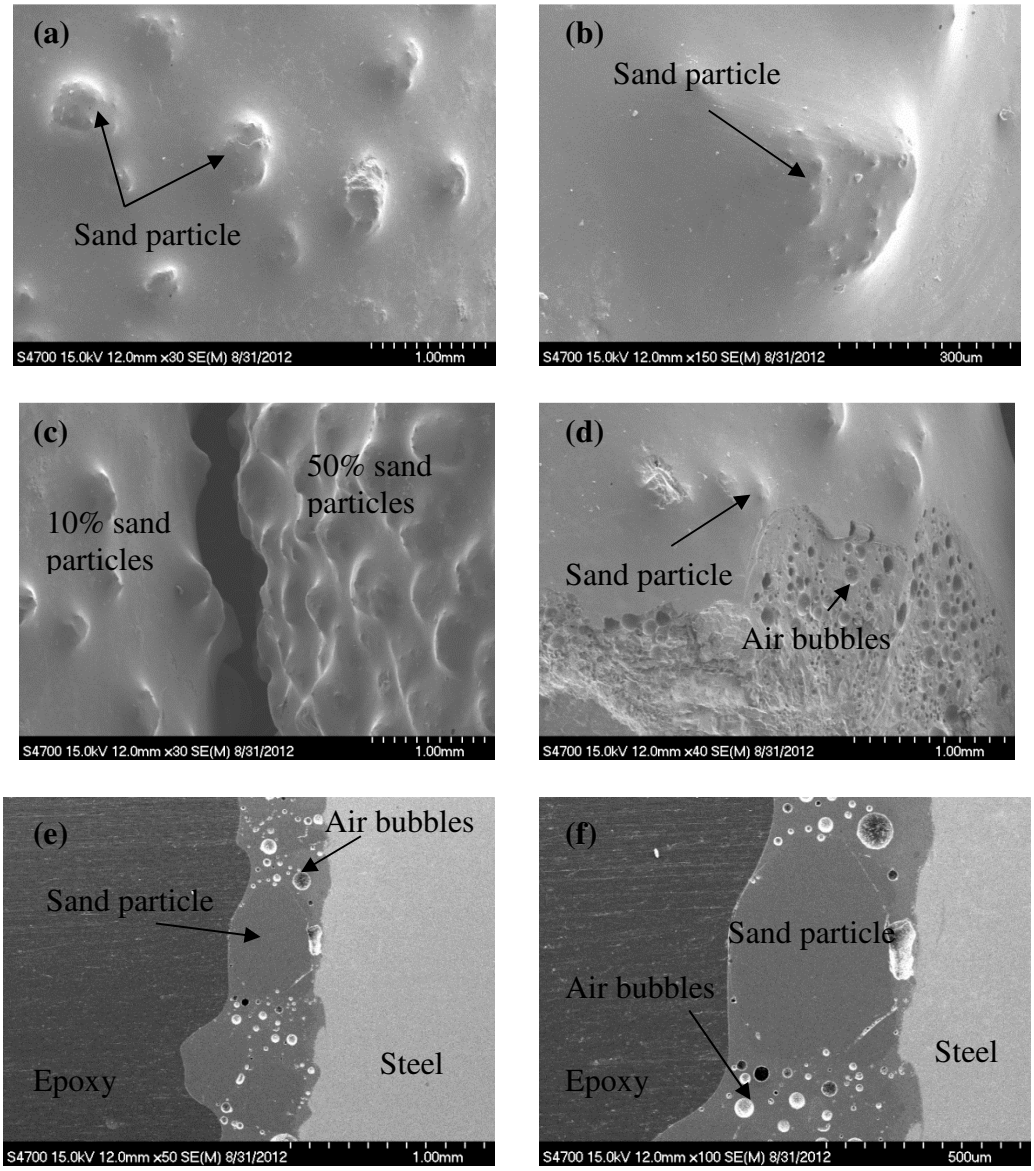

Fig.3. SEM images for (a-d) surface and (e-f) cross sectional morphologies of sand particle modified enamel coating. (a, b, and d: 10% sand particle; e and f: 50% sand particle)

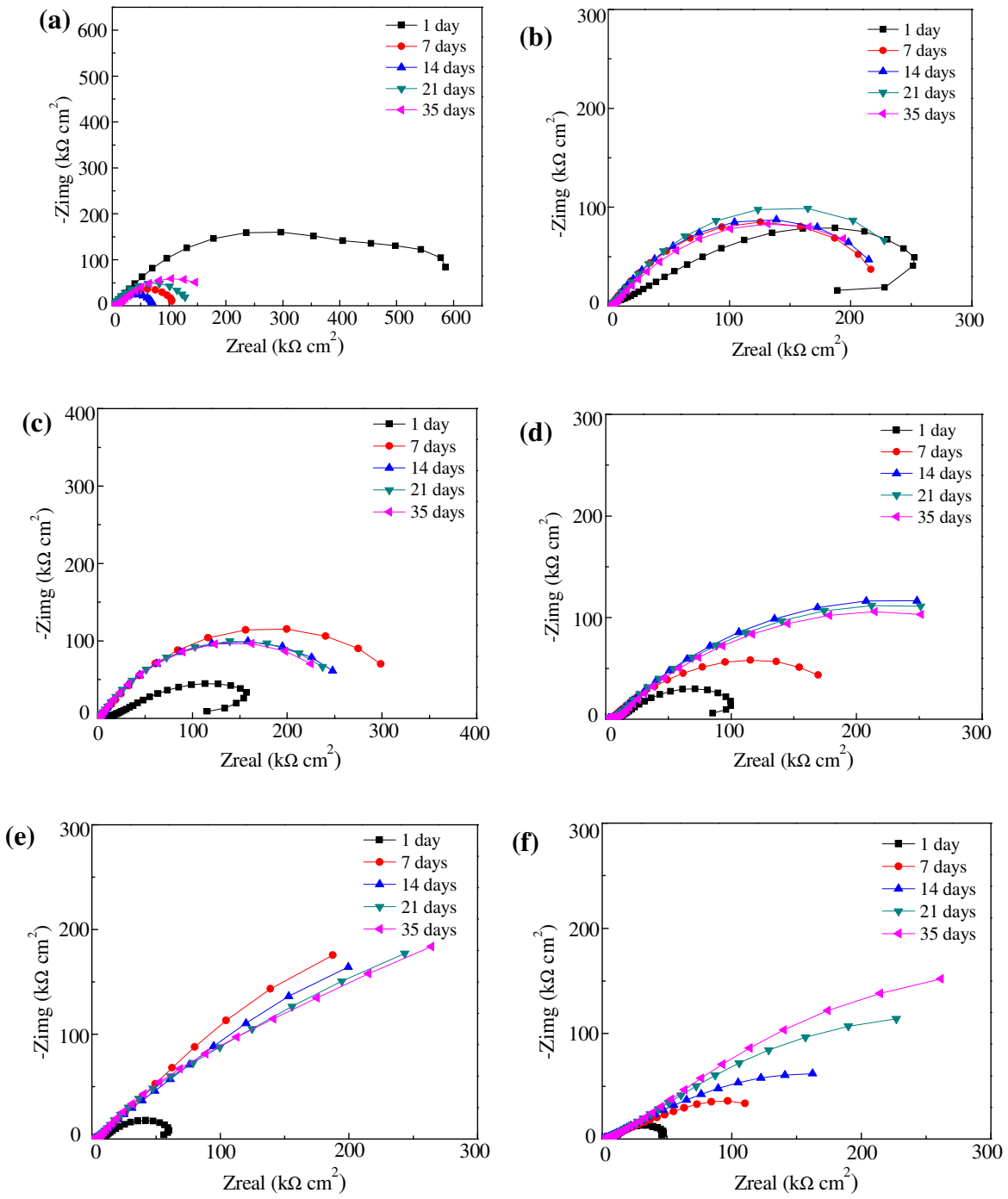

Fig.4. Typical EIS diagrams for sand particle modified enamel coating with different percentages of sand particle by weight: (a) 5%, (b) 10%, (c) 20%, (d) 30%, (e) 50%, and (f) 70%.

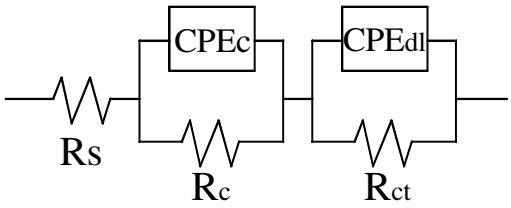

Fig.5. Equivalent electrical circuit model.

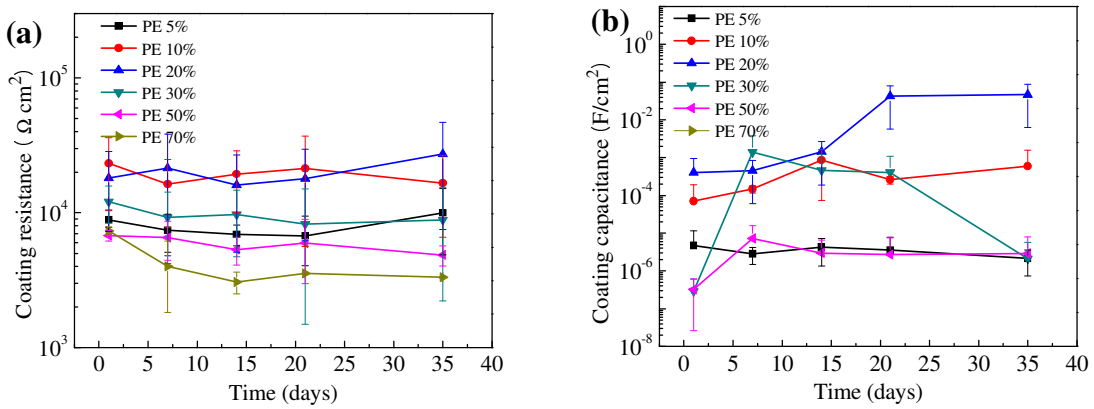

Fig.6. Coating properties evolution for: (a) coating resistance, and (b) coating capacitance.

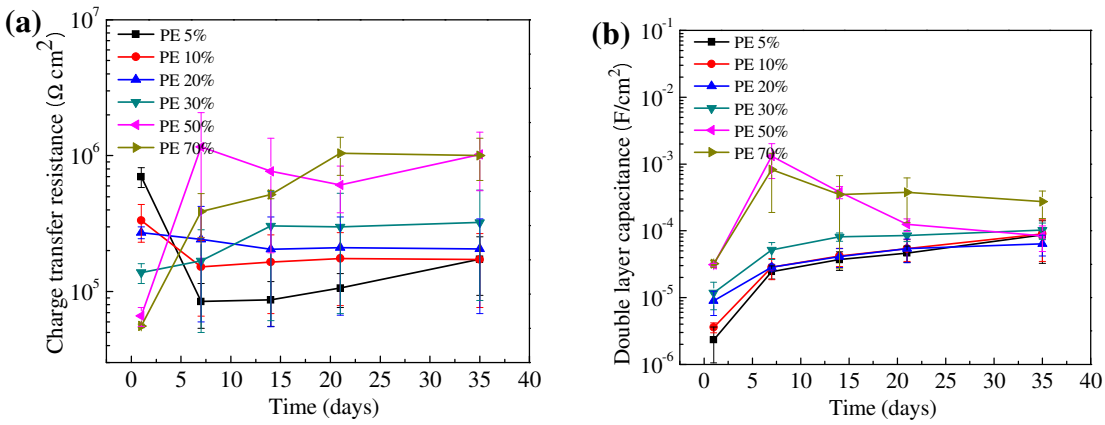

Fig.7. Corrosion properties evolution for: (a) charger transfer resistance, and (b) double layer capacitance.

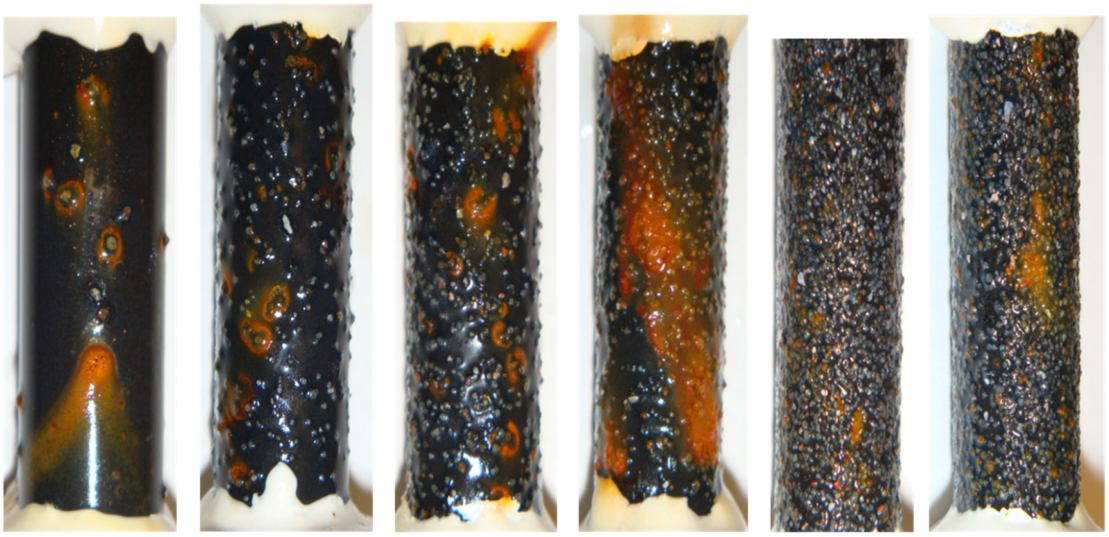

(a) **(b)** **(c)** **(d)** **(e)** **(f)**

Fig.8. Surface conditions of pure enamel coated steel bar with different sand particles after 35 days of corrosion testing: (a) 5%, (b) 10%, (c) 20%, (d) 30%, (e) 50%, and (f) 70%.

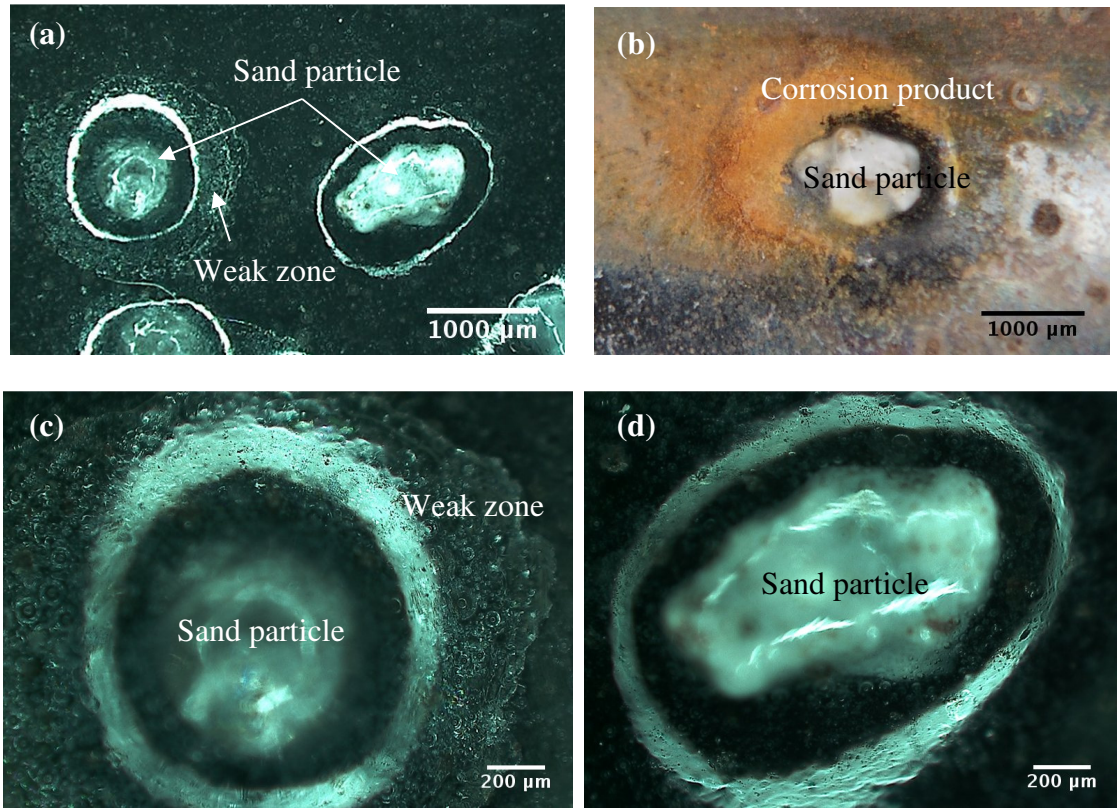

Fig.9. Surface observation for: (a) sand particle before corrosion test, (b) sand particle after corrosion test, (c) sand particle with weak zone before corrosion test, and (d) sand particle without weak zone before corrosion test.

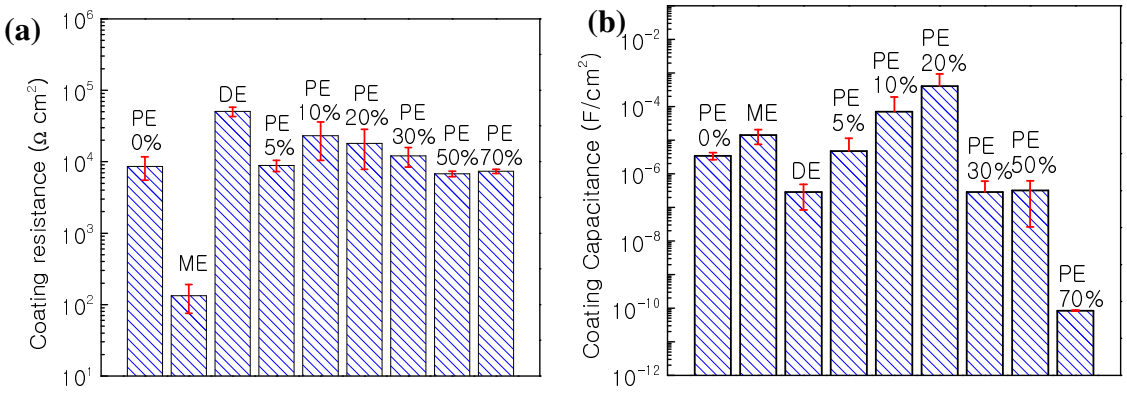

Fig.10. Comparison of coating properties with previous study [10]: (a) coating resistance, and (b) coating capacitance.

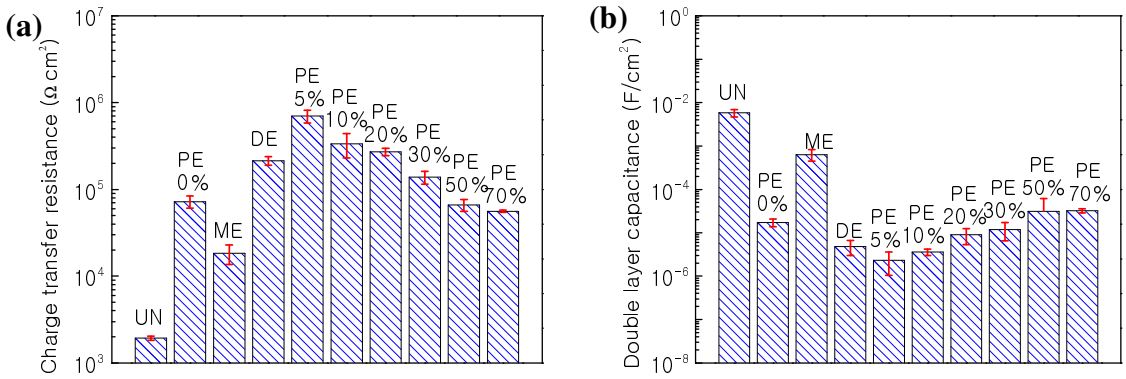

Fig.11. Comparison of corrosion properties with previous study [10]: (a) charger transfer resistance, and (b) double layer capacitance.

Table 1

Chemical composition of pure enamel

Materials	SiO_2	B_2O_3	Na_2O	K_2O	CaO	CaF_2	Al_2O_3	ZrO_2	CoO	MnO_2	NiO
Wt.%	44.0	19.3	15.8	2.8	0.0	4.7	4.6	5.3	0.9	1.5	1.0

Table 2

Chemical composition of steel bar

Element	C	Si	Mn	P	S	Cr	Mo	Ni	Co	Cu	V	Sn	Fe
Wt.%	0.43	0.22	0.95	0.15	0.07	0.17	0.03	0.10	0.01	0.46	0.02	0.02	97.37

3. SUMMARY AND CONCLUSIONS

Porcelain enamel is an alternative coating materials for reinforcement steel in concrete structures, because it has some advantages as follows. First, it has very stable chemical properties in harsh environments. Second, the properties of enamel are flexible and can be tailored for various applications. Third, it can chemically bond with the substrate steel. Lastly, as a coating, it can establish a physical barrier between steel bar and the corrosive environment.

For application of enamel coatings on reinforcement steel, there are two concerns. The first is the bond strength with surrounding concrete, and the second is the corrosion performance.

Addition of calcium silicate into the enamel coating could make it chemically react with surrounding concrete and form a strong area resulting in enhanced bond strength. However, addition of calcium silicate changed the microstructure of enamel coatings. Air bubbles in the pure enamel were released due to the connected channels formed by addition of calcium silicate. The connected channels provided paths for corrosive chemicals to penetrate and as a result, the corrosion resistance decreased significantly. These results are described in the first paper.

The primary constituent of sand particles is quartz, which is as the same as enamel coating. Therefore, addition of sand particles could be another option for enhanced bond strength and improved corrosion resistance. The increase of bond strength with concrete after adding sand particles was attributed to the increased surface roughness. Results in the second paper showed that the addition of sand particles did not change the microstructure of pure enamel coating significantly. Electrochemical tests also

demonstrated that the corrosion resistance of enamel coating modified by sand particle did not change significantly. Visual observation after corrosion test showed corrosion products surrounded some sand particles. This is because the sand particles used in this study were not uniform, some of them might have different coefficient of thermal expansion with enamel coating. Therefore, quality control is the key factor to increase the corrosion resistance further.

4. SUGGESTION FOR FUTURE WORK

Based on the findings and conclusions stated in the previous sections, future work on modified enamel coating should focus on the sand particles when applied to reinforcement steel both to enhance bond strength with concrete and to improve corrosion resistance. The addition of sand particles did not affect the corrosion resistance of enamel coatings. However, the surface roughness increased in comparison with pure enamel coating. The following suggestions are given in regards to the future work of enamel coating modified by sand particle applied to reinforcement steel for concrete:

1. The quality of sand particles used in the enamel coating should be strictly controlled. The corrosion resistance of enamel coating after being modified by these sand particles should be studied to make sure the problems found in this thesis could be solved.
2. The corrosion resistance of enamel coating modified by highly controlled sand particle should be investigated when they are embedded in concrete. Because the design of this coating is aimed to enhance the bond strength with concrete as well as to improve corrosion resistance of reinforcement steel in concrete. Concrete is the practical environment for this coating instead of pure salt solution.
3. The bond strength should be tested with different percentage of sand particles, as well as different size of sand particle. The amount of sand particle applied on the reinforcement steel surface is related to the surface roughness. When the amount of sand is small, the surface roughness is low; and when the amount of sand particles is great, the surface roughness is also low. Therefore, there is an optimum percentage of sand particles to reach the maximum surface roughness.

4. The corrosion resistance and bond strength should be tested when applied to deformed reinforcement steel bar, because the deformed steel bar is used widely instead of smooth steel bar. Rib deformation on the deformed steel bar would cause non-uniform coating thickness, and also reduce the height of the rib, both of which would affect the corrosion resistance and the bond strength.

APPENDIX

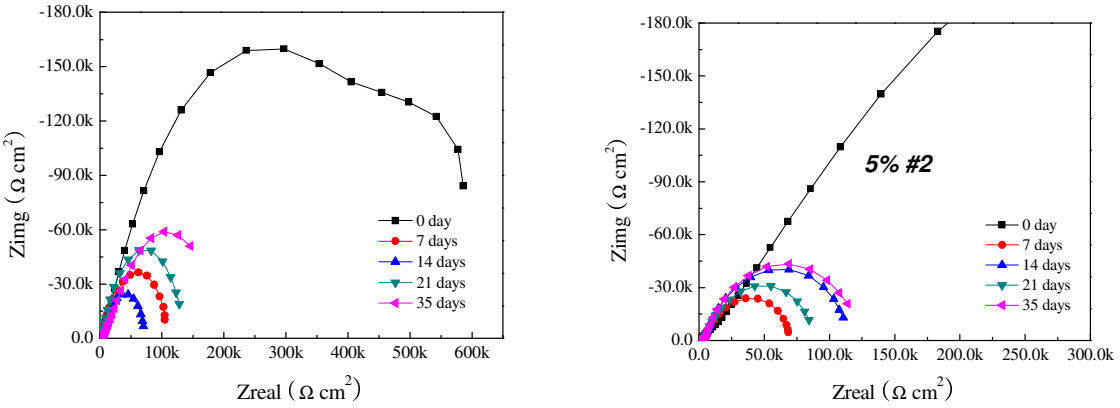

Figure 1: EIS results of pure enamel coating with 5% sand particles

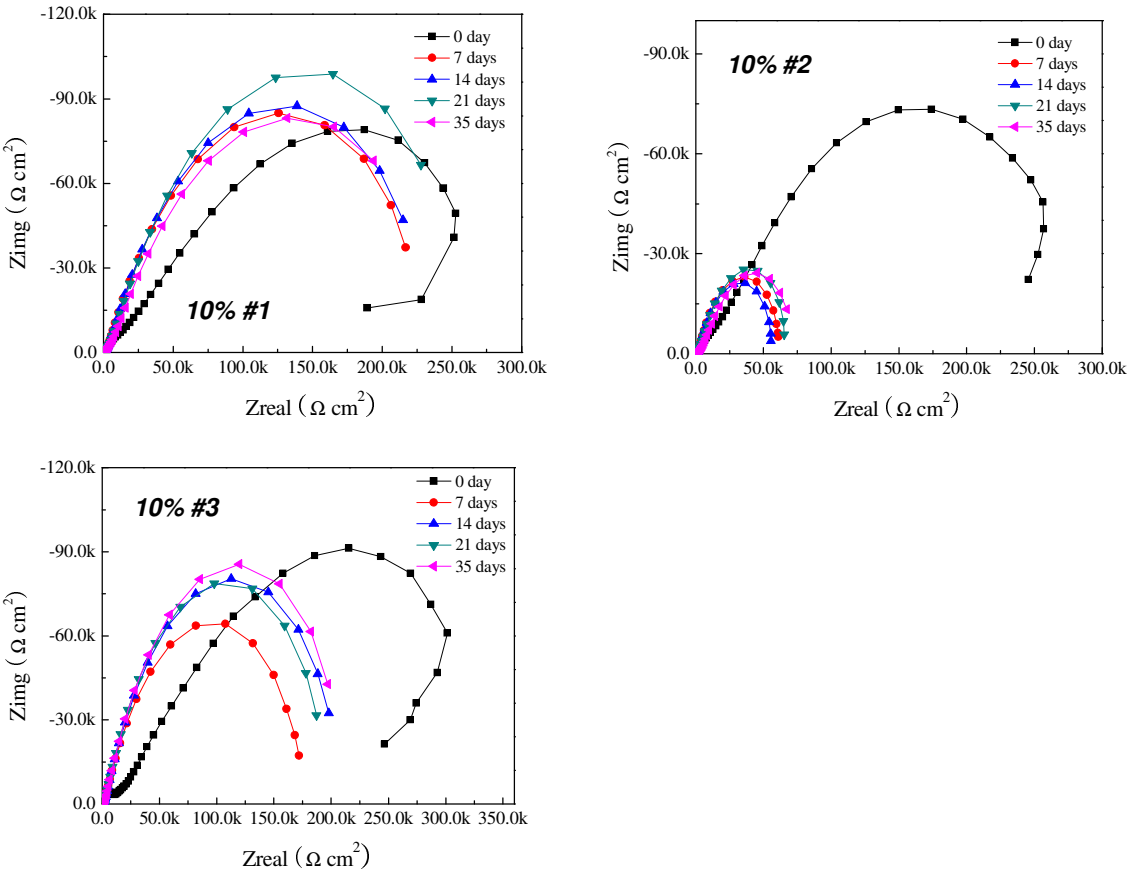

Figure 2: EIS results of pure enamel coating with 10% sand particles

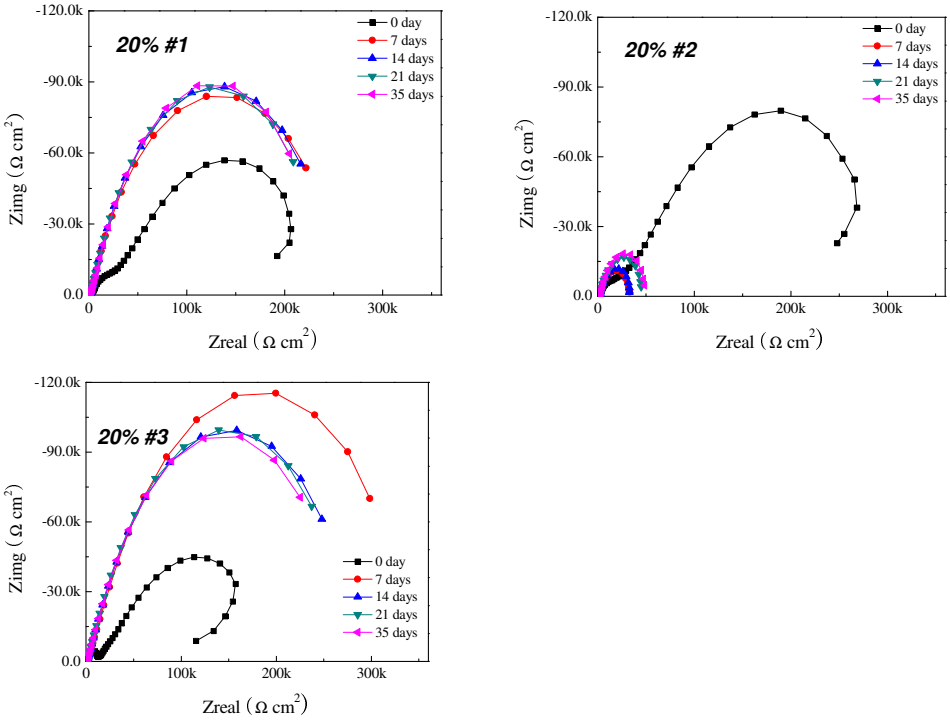

Figure 3: EIS results of pure enamel coating with 20% sand particles

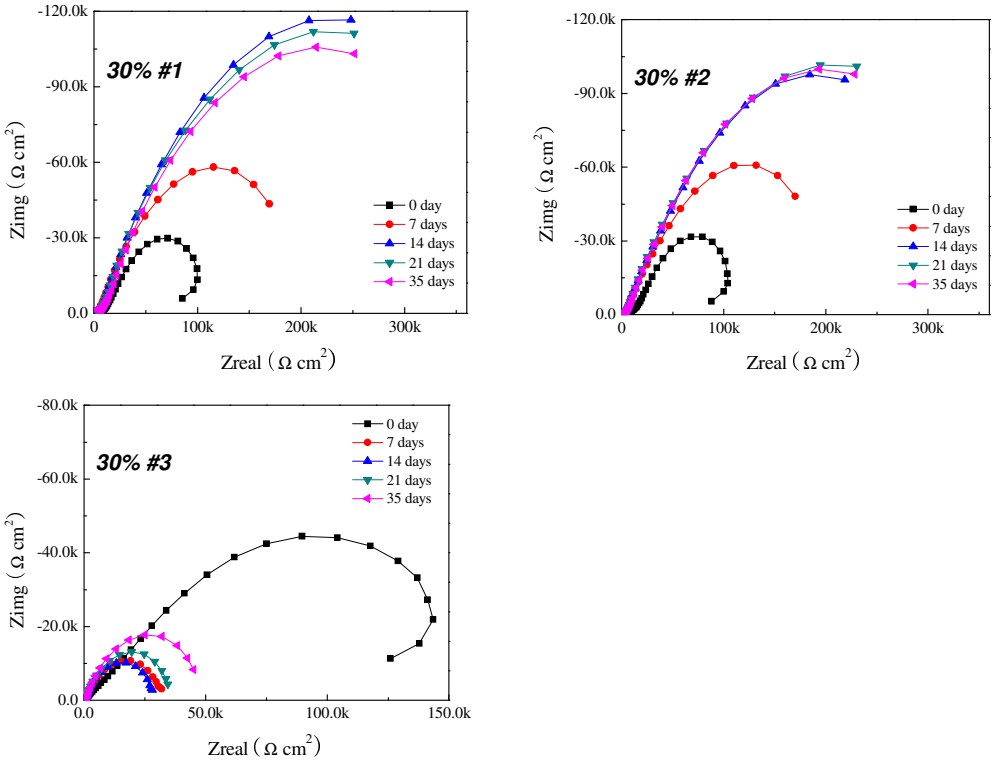

Figure 4: EIS results of pure enamel coating with 30% sand particles

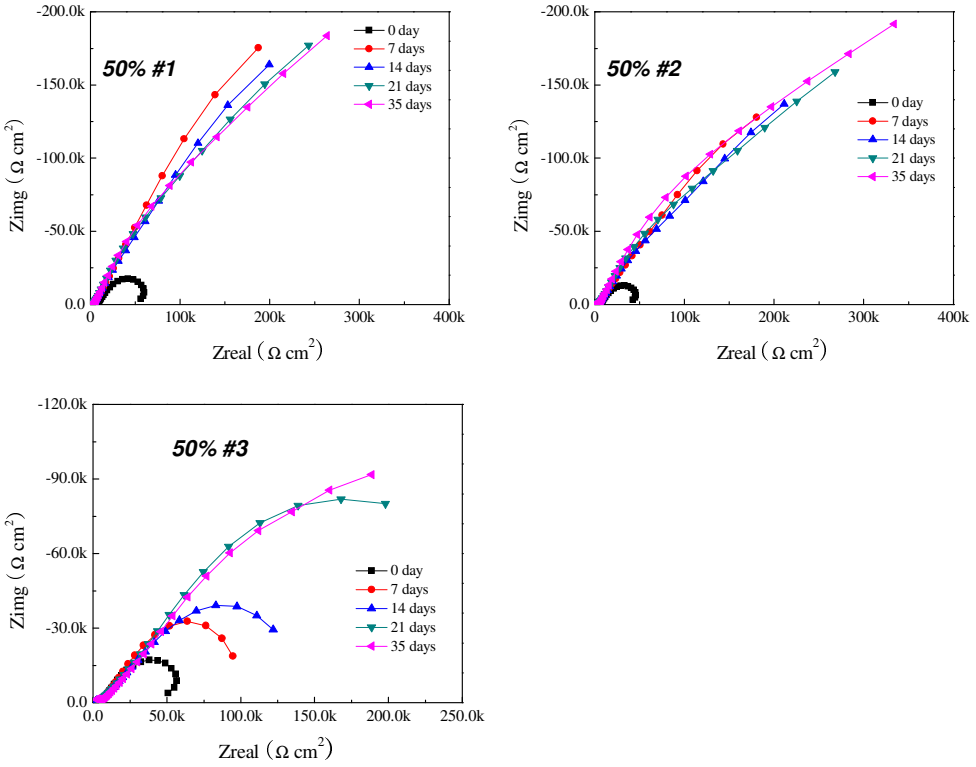

Figure 5: EIS results of pure enamel coating with 50% sand particles

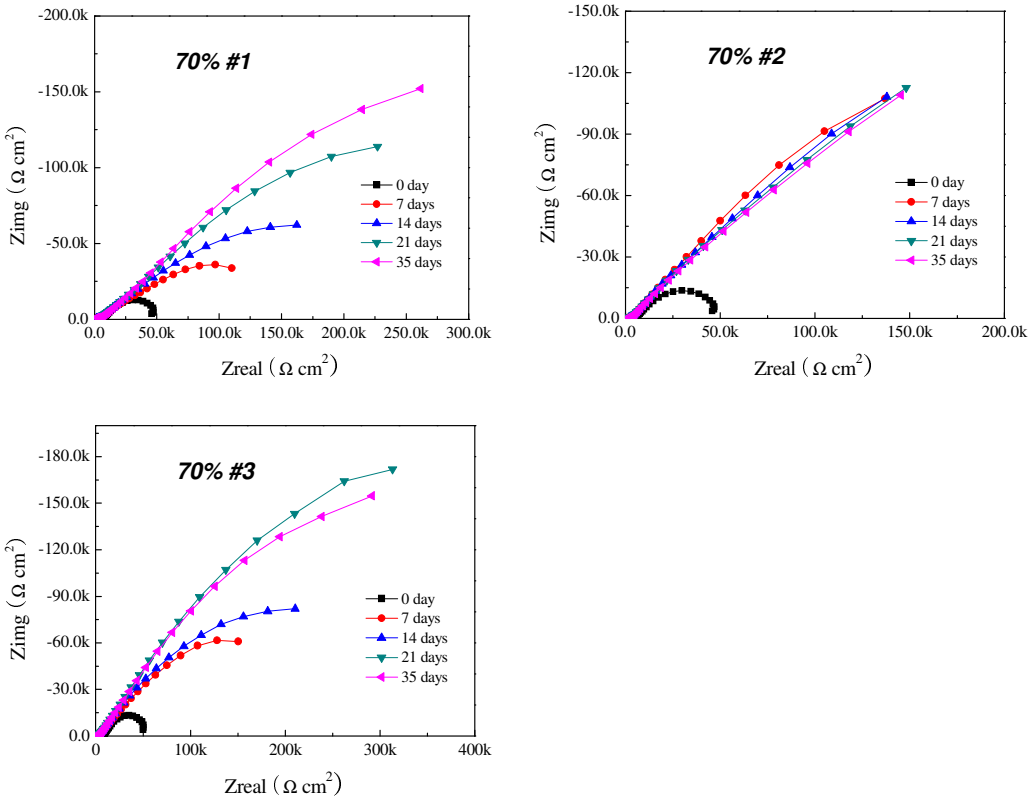

Figure 6: EIS results of pure enamel coating with 70% sand particles.

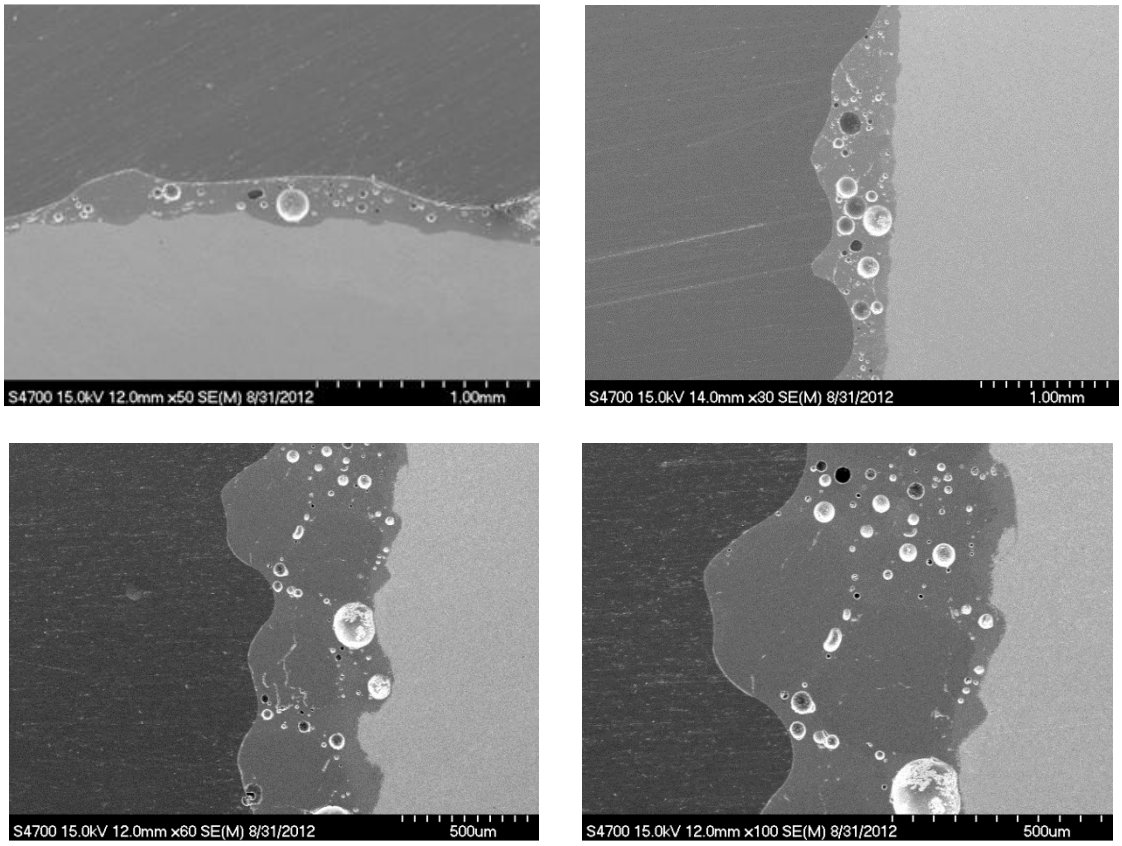

Figure 7: SEM images of enamel coating with sand particles

VITA

Fujian Tang was born in the City of Qufu, Shandong, China. After graduation from the high school affiliated with the Qufu Normal University in 2000, Fujian pursued a B.S. degree in Civil Engineering at the University of South China located in the City of Hengyang, Hunan, China. Upon graduation in 2004, he was directly admitted into Ph.D. Program in Civil Engineering at Hunan University under the supervision of Professor Weijian Yi due to his excellent academic performance. Four years later, he discontinued his PhD study in Hunan University and came to the U.S. In 2008, Fujian was admitted into PhD Program in Civil Engineering at Missouri University of Science and Technology under the supervision of Professor Genda Chen. In 2012, he decided to pursue a second graduate degree at the same time, M.S. Program in Materials Science and Engineering, under the supervision of Professor Richard K. Brow and Professor Genda Chen at Missouri University of Science and Technology. During his many years of graduate study both in China and in the U.S., he published 8 papers in international journals. In addition, four more are under review and three more are in preparation for potential publication. In December 2013, he received his Ph.D. degree in Civil Engineering from Missouri University of Science and Technology, Rolla, Missouri. In May 2014, he received his M.S. degree in Materials Science and Engineering from Missouri University of Science and Technology, Rolla, Missouri.